Primary Life Stage Boron Isotope and Trace Elements Incorporation in Aposymbiotic *Acropora millepora* Coral under Ocean Acidification and Warming

Henry C. Wu[1,2]*, Delphine Dissard[1], Florence Le Cornec[1], François Thil[2], Aline Tribollet[1], Aurelie Moya[3] and Eric Douville[2]

[1] Laboratoire d'Océanographie et du Climat (LOCEAN), IRD-Sorbonne Universités (UPMC, Université Paris 06), Centre National de la Recherche Scientifique-MNHN, IRD France-Nord, Bondy, France, [2] Laboratoire des Sciences du Climat et de l'Environnement, LSCE/IPSL, CEA-Centre National de la Recherche Scientifique-UVSQ, Université Paris-Saclay, Gif-sur-Yvette, France, [3] ARC Centre of Excellence for Coral Reef Studies, James Cook University, Townsville, QLD, Australia

Early-life stages of reef-building corals are vital to coral existence and reef maintenance. It is therefore crucial to study juvenile coral response to future climate change pressures. Moreover, corals are known to be reliable recorders of environmental conditions in their skeletal materials. Aposymbiotic *Acropora millepora* larvae were cultured in different seawater temperature (27 and 29°C) and pCO_2 (390 and 750 µatm) conditions to understand the impacts of "end of century" ocean acidification (OA) and ocean warming (OW) conditions on skeletal morphology and geochemistry. The experimental conditions impacted primary polyp juvenile coral skeletal morphology and growth resulting in asymmetric translucent appearances with brittle skeleton features. The impact of OA resulted in microstructure differences with decreased precipitation or lengthening of fasciculi and disorganized aragonite crystals that led to more concentrations of centers of calcifications. The coral skeletal $\delta^{11}B$ composition measured by laser ablation MC-ICP-MS was significantly affected by pCO_2 ($p = 0.0024$) and water temperature ($p = 1.46 \times 10^{-5}$). Reconstructed pH of the primary polyp skeleton using the $\delta^{11}B$ proxy suggests a difference in coral calcification site and seawater pH consistent with previously observed coral pH up-regulation. Similarly, trace element results measured by laser ablation ICP-MS indicate the impact of pCO_2. Primary polyp juvenile Sr/Ca ratio indicates a bias in reconstructed sea surface temperature (SST) under higher pCO_2 conditions. Coral microstructure content changes (center of calcification and fasciculi) due to OA possibly contributed to the variability in B/Ca ratios. Our results imply that increasing OA and OW may lead to coral acclimation issues and species-specific inaccuracies of the commonly used Sr/Ca-SST proxy.

Keywords: ocean acidification, $\delta^{11}B$, pH proxy, Sr/Ca, sea surface temperature proxies, scleractinian corals, *Acropora millepora*, laser ablation

INTRODUCTION

Scleractinian corals, the building blocks of coral reefs in the tropical oceans, are known for the formation of extremely productive and diverse ecosystems. These marine calcifying organisms are however threatened and in most areas in decline. The results of increasing anthropogenic CO_2 emissions are elevated sea surface temperatures (SST) and decreases in ocean pH (e.g., Pandolfi et al., 2011). Ocean acidification (OA) is the process by which the oceans take up atmospheric anthropogenic CO_2 leading to an increase in seawater H^+ concentrations and consequently decrease in pH (Caldeira and Wickett, 2003). The effects of ocean warming or thermal stress have been widely documented in coral reefs around the world by mass coral bleachings and mortalities that are becoming more frequent and severe (Hoegh-Guldberg et al., 2007; Eakin et al., 2009; Pandolfi et al., 2011). Not only is warming impacting corals worldwide, but the effect of OA can also affect coral calcification (Gattuso et al., 1999; Kleypas et al., 1999; Anthony et al., 2008).

Declines in coral calcification over multi-decadal timescales have already been observed (De'ath et al., 2009) with further decreases projected under future climate change scenarios (Orr et al., 2005; Pandolfi et al., 2011). Reduced skeletal growth under OA conditions has been documented in corals in both natural and artificial environments (Kuffner et al., 2008; Cohen et al., 2009; Kroeker et al., 2010; Fabricius et al., 2011). Complicating the full understanding of future OA effects on ecosystems is the fact that responses vary among species; with some coral species being more resilient and less affected than others (Fabricius et al., 2011; Edmunds et al., 2012). Studies have also shown enhanced anomalous coral calcification in natural OA settings due to the combined effects of ocean warming (OW) and OA (Rodolfo-Metalpa et al., 2011).

In addition to the threat on adult corals, OA and OW can affect early-life stages of reef building species hindering coral reef sustainability. Physiological studies have shown that OA impaired coral larval metamorphosis, negatively impacted recruitment, and induced deformities in juvenile coral skeletons (Albright et al., 2010; Nakamura et al., 2011; Doropoulos et al., 2012; Foster et al., 2015, 2016). Other studies have however documented conflicting biologically-related responses such as disrupted gene expression and tolerance to the combined effects of OA and OW in juveniles or recently metamorphosed coral larvae (Moya et al., 2012; Rivest and Hofmann, 2014; Baria et al., 2015). Important questions remain for post-metamorphosis juvenile corals because studies have shown remarkable adaptability without significant effects linked to OA and OW (Chua et al., 2013a,b). Furthermore, changes in juvenile skeletal formation and geochemistry continue to be relatively unknown and unresolved.

In this study, we examined the primary polyp of the branching coral *Acropora millepora* to understand the effects of OA and OW on skeletal formation and geochemistry under end-of-century emission scenarios (Field et al., 2014). Our coral culture experiment provides a novel opportunity to acquire information on coral response to climate change because *A. millepora* have been shown to be the emerging coral model to study coral habitat

degradation (Humphrey et al., 2008), elevated temperature stress (Meyer et al., 2011), genetic response to survival of combined thermal and acidification stress (Rocker et al., 2015), and possible adaptation to OA (Moya et al., 2015).

One possible tool to observe OA and the associated seawater pH change is based on the $\delta^{11}B$ composition of marine calcifiers (Hershey et al., 1986; Hemming and Hanson, 1992). The relative abundance of the two boron species in seawater, boric acid, $B(OH)_3$, and borate, $B(OH)_4^-$, is pH dependent. Moreover, the isotopic composition and the isotopic equilibrium fractionation between the two aqueous boron species (boric acid and borate) are also pH dependent (Hershey et al., 1986; Hemming and Hanson, 1992). Based on the assumption that marine carbonates reflect the isotopic composition of $B(OH)_4^-$ (Spivack et al., 1993; Palmer and Pearson, 2003), the $\delta^{11}B$ signature of marine biocarbonates such as coral aragonite skeleton have been shown to reflect seawater pH (Hönisch et al., 2004; Pelejero et al., 2005; Wei et al., 2009; Douville et al., 2010; D'Olivo et al., 2015).
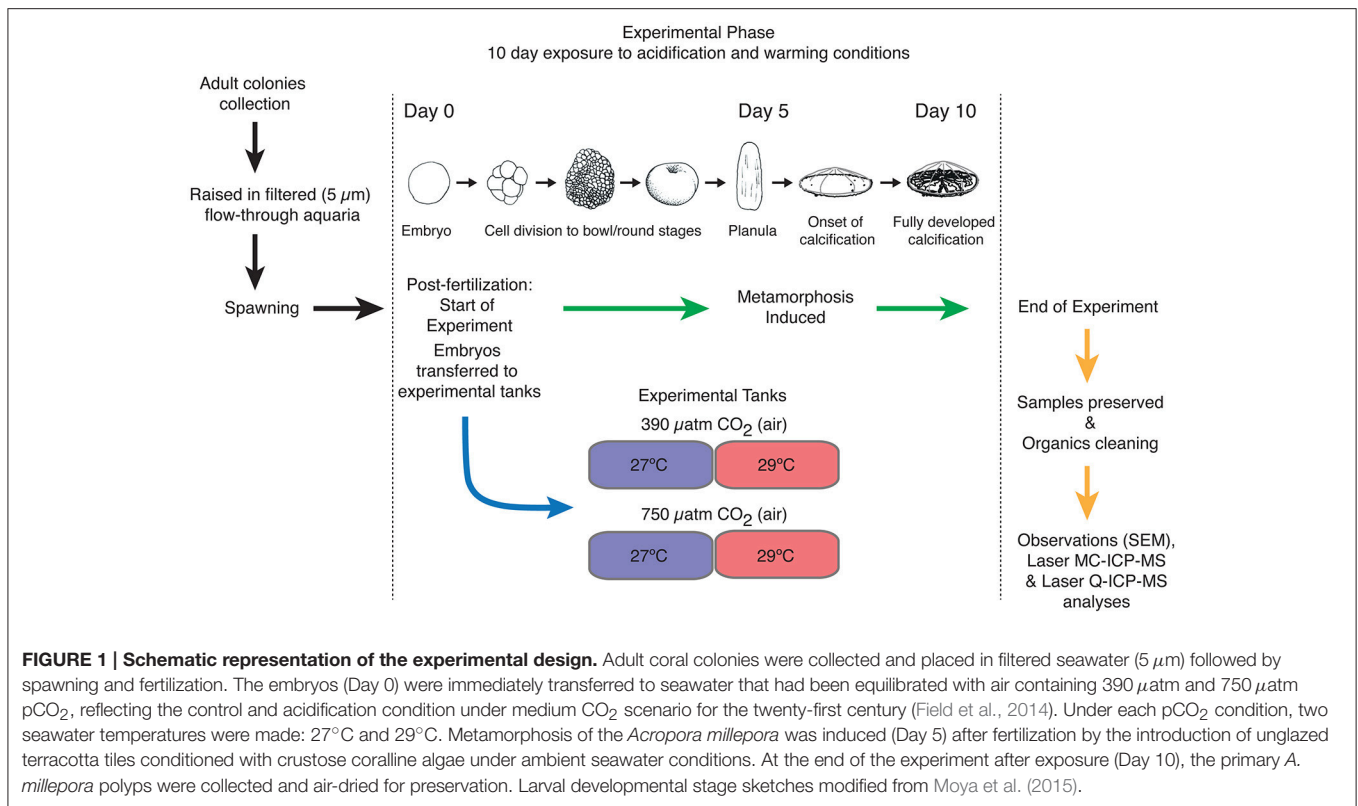
The aragonite skeleton of reef-building corals such as *Porites* spp. and *Acropora* spp. have been shown to be reliable recorders of climate (e.g., SST, $\delta^{18}O$ of seawater, etc.) (Dunbar and Wellington, 1981; Corrège, 2006; Tierney et al., 2015; Sadler et al., 2016). Coral skeletal Sr/Ca ratios are widely used for SST reconstructions with success (see reviews and compilations in Corrège, 2006; Tierney et al., 2015). The strong influence of SST on coral B/Ca and the U/Ca ratios at certain locations has also been documented (Sinclair et al., 1998; Fallon et al., 1999, 2003; Cardinal et al., 2001; Felis et al., 2010). The branching coral genus *Acropora* can be considered an ideal candidate for climate reconstructions because of its wide spatial distribution across the tropical oceans with long temporal range from the early-Holocene to today (Ribaud-Laurenti et al., 2001; Sadler et al., 2014). Using *in situ* laser ablation geochemical analyses, we measured the $\delta^{11}B$ and trace element (B/Ca, Sr/Ca, U/Ca) signatures of juvenile *A. millepora* (primary polyps). We aim to shed more light on the systematics and incorporation of the commonly used coral-based climate proxies in juvenile primary skeleton under the effects of OA and OW.

MATERIALS AND METHODS
Experimental Setup

Fifteen adult colonies of *A. millepora* were collected off the coast of Orpheus Island, Australia (under GBRMPA permit No G10/33174.1) and transported within 3 h to the Marine and Aquaculture Research Facilities Unit (MARFU) at James Cook University in Townsville, Australia. The colonies were maintained in outdoor flow-through aquaria filled with 5 μm filtered seawater resulting in the absence of zooxanthellae endosymbionts for coral colonization (**Figure 1**). The exclusion of these microorganisms limits our impact observations to the coral host animal itself without the complications of zooxanthellate endosymbionts involvement (e.g., photosynthesis, lipids production, etc.).

Immediately after spawning, eggs and sperm were collected and transferred into fertilization tanks. Once fertilized (i.e., 2-cell stage), the embryos were transferred and kept for 10 consecutive

FIGURE 1 | Schematic representation of the experimental design. Adult coral colonies were collected and placed in filtered seawater (5 μm) followed by spawning and fertilization. The embryos (Day 0) were immediately transferred to seawater that had been equilibrated with air containing 390 μatm and 750 μatm pCO$_2$, reflecting the control and acidification condition under medium CO$_2$ scenario for the twenty-first century (Field et al., 2014). Under each pCO$_2$ condition, two seawater temperatures were made: 27°C and 29°C. Metamorphosis of the *Acropora millepora* was induced (Day 5) after fertilization by the introduction of unglazed terracotta tiles conditioned with crustose coralline algae under ambient seawater conditions. At the end of the experiment after exposure (Day 10), the primary *A. millepora* polyps were collected and air-dried for preservation. Larval developmental stage sketches modified from Moya et al. (2015).

days in experimental tanks that were previously equilibrated at four different conditions. The four experimental conditions were as follows: (1) 390 μatm pCO$_{2\,(air)}$ at 27°C (control condition), (2) 390 μatm pCO$_{2\,(air)}$ at 29°C, (3) 750 μatm pCO$_{2\,(air)}$ at 27°C, and (4) 750 μatm pCO$_{2\,(air)}$ at 29°C. CO$_2$ concentration was produced and regulated using a CO$_2$ mixing system developed by Munday et al. (2009). A schematic summary of the experimental setup can be found in **Figure 1**.

All seawater measurements such as pH (NBS scale, Hach HQ11D, calibrated daily), temperature (°C), and Total Alkalinity (A$_T$) were monitored daily at 11:00 over the duration of the experiment. Mean seawater chemistry parameters [pCO$_{2\,(seawater)}$, carbonate ion (CO$_3^{2-}$), and aragonite saturation state ($\Omega_{Aragonite}$)] were estimated using CO2SYS version 2.1 (Lewis and Wallace, 1998) with salinity of 35 using dissociation constants from Mehrbach et al. (1973) and refitted by Dickson and Millero (1987) with boron source of Uppstrom (1974) (**Table 1**).

Metamorphosis of the *A. millepora* larvae into coral juveniles of a single corallite or primary polyp juveniles occurred within the water column of the aquaria after 5 days leading to fully developed calcification over the duration of the experiment (**Figure 1**). Metamorphosis was induced by the introduction of unglazed autoclaved terracotta tiles that had been conditioned with crustose coralline algae under ambient seawater conditions (Heyward and Negri, 1999). After 10 days of exposure to experimental conditions (5 days post-metamorphosis), the coral juveniles from the four experimental conditions were collected (**Figure 1**). The samples were left to dry in sample tubes at room

temperature and transported to Laboratoire d'Océanographie et Climat (LOCEAN) at the Institut de Recherche pour le Développement (IRD) Centre France-Nord in Bondy, France.

A. millepora primary polyp juveniles were randomly picked from each individual experimental condition and pretreated with 50% NaOCl for up to 72 h to remove the organic matter (coral tissues). The primary polyp juveniles were then placed in 18.2 MΩ Milli-Q water for cleaning overnight. Pretreatment of samples by NaOCl is a common procedure that has no influence on microstructure and trace element or boron isotope geochemistry (Watanabe et al., 2001; Nothdurft and Webb, 2007; Holcomb et al., 2015).

Laser Ablation—ICP-MS and—MC-ICP-MS Analyses

Trace element analyses on the cleaned primary polyp juveniles were completed by laser ablation (ESI NWR-213nm; Nd:YAG Laser) coupled to an Agilent 7500cx Quadrupole Inductively Coupled Plasma Mass Spectrometer (LA-ICP-MS) on the ALYSES Analytical Platform (IRD/UPMC) at LOCEAN. Trace element measurements by LA-ICP-MS has been shown to be both precise and accurate at the micron-scale (Sinclair et al., 1998; Fallon et al., 1999). This technique was chosen for this study because of the limited size and number of primary polyp juvenile corals. The operational repetition rate frequency of the laser was 10 Hz and 5 mJ for laser power with sample introduction to the ICP-MS by helium mixed with argon prior to reaching the plasma torch (**Table 2**). Each LA-ICP-MS analysis was completed as a single laser spot of 40 μm (beam diameter) on the surface of the

TABLE 1 | *Acropora millepora* **juvenile coral experimental conditions and parameters.**

Condition	Target pCO_2 (air) (ppm)	Measured parameters			CO2SYS calculated parameters			
		Temp (°C)	pH (NBS scale)	A_T (μmol kg^{-1})	pH (Total scale)	pCO_2 (seawater) (μatm)	CO_3^{2-} (μmol kg^{-1})	$\Omega_{Aragonite}$
1	390	26.6 ± 0.2	8.08 ± 0.07	1947.4 ± 34.0	7.94 ± 0.07	448.43 ± 78.48	157.01 ± 21.17	2.51 ± 0.34
2	390	28.9 ± 0.1	8.08 ± 0.07	1955.7 ± 50.3	7.94 ± 0.07	457.69 ± 95.28	166.46 ± 23.01	2.69 ± 0.37
3	750	26.6 ± 0.2	7.93 ± 0.06	1920.4 ± 60.3	7.79 ± 0.06	665.96 ± 81.15	115.79 ± 16.68	1.85 ± 0.27
4	750	29.0 ± 0.2	7.94 ± 0.10	1911.1 ± 53.9	7.79 ± 0.10	671.43 ± 160.05	125.24 ± 27.39	2.03 ± 0.44

Seawater parameter values from 10 daily measurements and as calculated by CO2SYS (Lewis and Wallace, 1998). Daily measurements of temperature (°C), pH, and Total Alkalinity (A_T) monitored at 11:00 for 10 days. The pH measurements were made by the Hach HQ11D on the National Bureau of Standards scale and converted to Total scale using the CO2SYS software. CO2SYS version 2.1 (Lewis and Wallace, 1998) was used to estimate seawater chemistry: pCO_2 of seawater (pCO_2 (seawater)), carbonate ion CO_3^{2-}), and aragonite saturation ($\Omega_{Aragonite}$) based on salinity of 35 using dissociation constants from Mehrbach et al. (1973) and refitted by Dickson and Millero (1987) with boron source of Uppstrom (1974). All values are given as the calculated mean of each condition (daily measurements and CO2SYS conversions) as well as the standard deviation of the calculated mean.

TABLE 2 | Laser ablation ICP-MS and MC-ICP-MS instrumental setup.

Analysis	Repetition rate frequency (Hz)	Laser energy (mJ)	Laser spot size (μm)	Dwell time (sec)	Washout time (sec)
ICP-MS	10	5	40	50	60
MC-ICP-MS	15	7	100	60	40

Summary of the laser ablation ICP-MS and MC-ICP-MS analyses instrumental setup. The operational repetition rate or laser frequency is in Hz and laser energy is in mJ. The laser spot size is the laser beam diameter in μm, the dwell time is the acquisition time of laser sampling in seconds, and washout time is the clearance time between individual laser spot analysis in seconds.

primary polyp juvenile with a laser dwell time (acquisition time) of 50 s. Washout time between each laser spot analysis was 60 s (**Table 2**). Eight seconds of gas blank was measured before the initiation of each laser analysis. Daily adjustments of the LA-ICP-MS were done using the NIST SRM 610 standard (glass matrix standard reference material).

The δ^{11}B ratio analysis on the same samples were performed by laser ablation (ESI NWR-193 nm; ATLEX 300SI Laser) coupled to a Thermo Scientific Neptune Plus Multi-Collector ICP-MS (LA-MC-ICP-MS) at the Laboratoire des Sciences du Climat et de l'Environnement (LSCE), Gif-sur-Yvette, France. The thorough laser application δ^{11}B ratio analysis methodology including accuracy and precision using this instrumentation has been previously documented on a *Porites* sp. coral (Thil et al., 2016). The laser spot mode was used with a repetition rate frequency of 15 Hz, 7 mJ for laser energy, beam diameter of 100 μm, and a laser dwell time of 60 s (**Table 2**). Washout time between each laser spot analysis was 40 s (**Table 2**). Daily adjustments of the LA-MC-ICP-MS were optimized using the NIST SRM 612 standard (glass matrix standard reference material).

Each primary polyp juvenile was analyzed at three carefully chosen locations on the skeleton for trace elements determination and three additional locations for δ^{11}B signature (6 total laser spot analyses per juvenile). The laser was triggered on a location where at least 90% of the laser field contained skeletal material to have a more robust analytical signal because the primary polyp (single corallite) juveniles are porous (**Figure 2**). The total number of juveniles analyzed varied between conditions, with a minimum of 10 individuals per
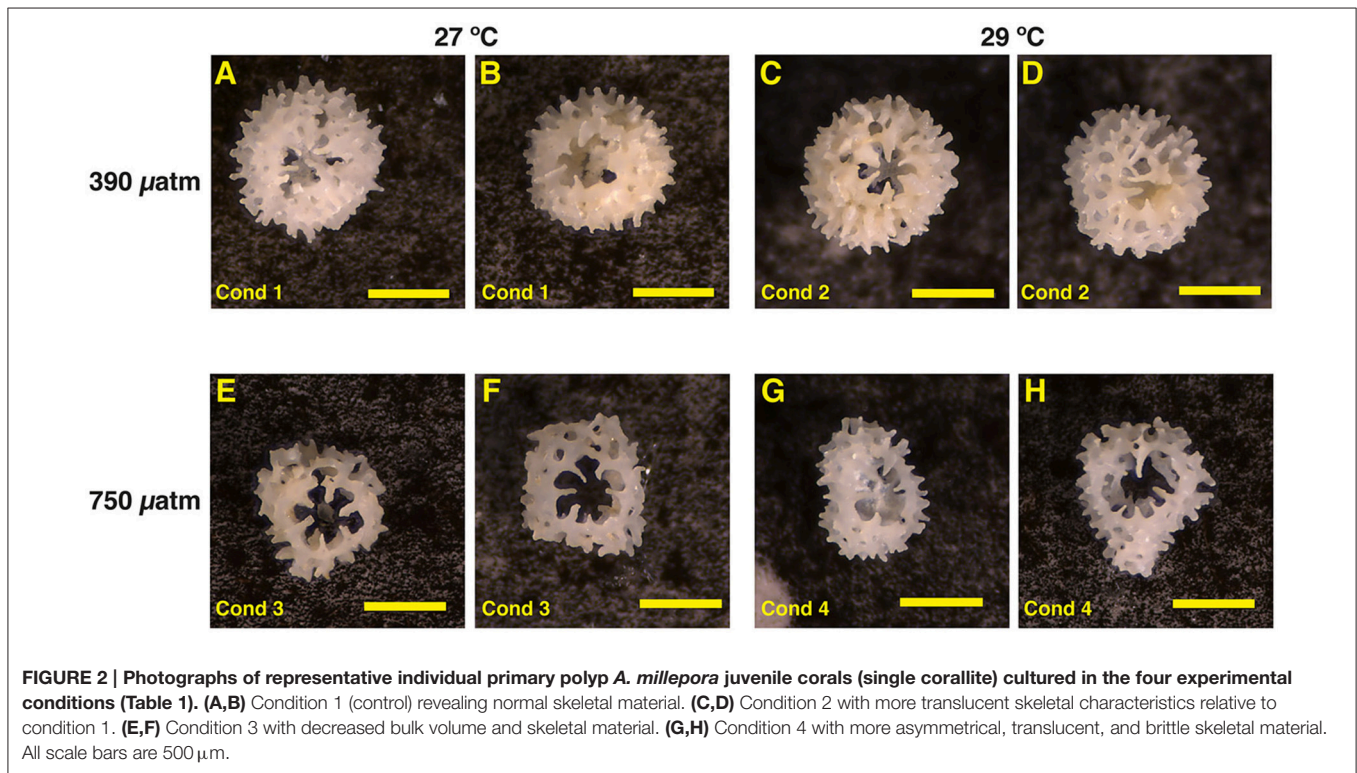
condition, producing a minimum of 30 trace element and 30 δ^{11}B ratio measurements per condition.

The main criteria for our laser ablation results were: (a) each juvenile must have three complete laser spots, (b) each laser spot's analytical signal is constant over time, and (c) each measurement is above the limits of detection for the investigated element. Results for an individual juvenile were rejected if there was an incomplete measurement from any of the three laser spots. With these criteria for trace elements, 15 juveniles were analyzed for condition 1 (number of laser spots, $n = 45$), 22 for condition 2 ($n = 66$), 20 for condition 3 ($n = 60$), and 22 for condition 4 ($n = 66$). For the δ^{11}B ratio, 10 juveniles were analyzed for condition 1 (number of laser spots, $n = 30$), 10 for condition 2 ($n = 30$), 14 for condition 3 ($n = 42$), and 13 for condition 4 ($n = 39$).

Repeated measurements of the international standards NIST SRM 610 (trace elements) or NIST SRM 612 (boron isotopes) were completed under the same conditions (e.g., laser spot size, frequency, etc.) for instrumental drift correction and precision assessment and verification. The inter-laboratory calibration coral standard JCp-1 (*Porites* coral) (Okai et al., 2002; Hathorne et al., 2013) was also measured for comparison. Measurements of the JCp-1 sample was derived from pressed individual pellets made of 500 mg of JCp-1 powder under a 10 ton cm^{-2} force following the description of Lazareth et al. (2007). Additionally, a *Porites* sp. coral section of known δ^{11}B ratio (Thil et al., 2016) was also repeatedly measured on the MC-ICP-MS for baseline verification.

Daily LA-ICP-MS data processing and correction for machine drift was completed using the GLITTER software (Van Achterbergh et al., 2001). We chose the most stable signal integration time (15–40 s) with ^{43}Ca as the internal standard with 40 wt % Ca content and gas blank removed from each signal. The NIST SRM 610 glass standard was used as the external standard to calculate quantitative element concentration of the unknown coral juveniles using concentrations of Pearce et al. (1997).

LA-ICP-MS results are presented in element/Ca ratios for conventional coral geochemistry-based paleoclimatology comparison. LA-ICP-MS precision of NIST SRM 610 is within the certified/suggested values and reported errors in Pearce et al. (1997) (mean $\pm$ 1σ standard deviation, SD; % relative standard deviation, RSD): 17.402 ± 0.394 mmol mol^{-1} for B/Ca (2.27%

FIGURE 2 | Photographs of representative individual primary polyp A. millepora juvenile corals (single corallite) cultured in the four experimental conditions (Table 1). (A,B) Condition 1 (control) revealing normal skeletal material. **(C,D)** Condition 2 with more translucent skeletal characteristics relative to condition 1. **(E,F)** Condition 3 with decreased bulk volume and skeletal material. **(G,H)** Condition 4 with more asymmetrical, translucent, and brittle skeletal material. All scale bars are 500 μm.

RSD), 3.041 ± 0.032 mmol mol^{-1} for Sr/Ca (1.06% RSD), and 1031.823 ± 14.809 μmol mol^{-1} for U/Ca (1.43% RSD). Repeated analysis of the international coral standard JCp-1 (carbonate powder) pressed pellet for trace elements are 0.577 ±0.056 mmol mol^{-1} for B/Ca (9.67% RSD), 9.484 ± 0.266 mmol mol^{-1} for Sr/Ca (2.81% RSD), and 1.233 ± 0.109 μmol mol^{-1} for U/Ca (8.27% RSD). The published robust average and SD of the JCp-1 standard measured in solution are 0.459 ± 0.022 mmol mol^{-1} for B/Ca, 8.838 ± 0.042 mmol mol^{-1} for Sr/Ca, and 1.192 ± 0.045 μmol mol^{-1} for U/Ca (Hathorne et al., 2013). The inter-laboratory offset and larger SD of the JCp-1 standard is due to differences in analytical techniques between solution- and laser ablation-based measurements. No corrections were applied to our results with the published values of JCp-1 because of (a) the large heterogeneity of the powder pellet analyzed under laser ablation compared to solution-based results and (b) our goal to focus on the relative changes and differences between experimental conditions and not in the reconstruction of absolute SST.

The δ^{11}B ratio LA-MC-ICP-MS analysis results are reported in ‰ deviation compared to the published JCp-1 value (24.3‰) as reference (Foster et al., 2013) allowing us to obtain a low 2σ SD (±0.38‰; $n = 47$) within the published 2σ SD. The 2σ SD of repeated analyses of the international certified NIST SRM 612 silicate glass matrix (Brand et al., 2014) was ±0.88‰ ($n = 23$). The analyzed internal laboratory standard (Porites coral slab section) δ^{11}B ratio was homogeneous (20.69‰) with a low 2σ SD (±0.47‰; $n = 47$). Daily data processing and correction were based on a combination of our in-house Porites sp. sample (Thil et al., 2016) and the JCp-1 standard.

Estimation of Seawater pH and Statistical Analyses

The estimation of seawater pH values (Total scale) was calculated from the primary polyp juvenile δ^{11}B ratios following established equation (e.g., Zeebe et al., 2001).

$$pH_{sw} = pK_B - \log\left[\left(\delta^{11}B_{sw} - \delta^{11}B_c\right)/\right.$$
$$\left.\left\{\alpha_{[B3-B4]}\delta^{11}B_c - \delta^{11}B_{sw} + 10^3\left(\alpha_{[B3-B4]} - 1\right)\right\}\right]$$

The parameters of Equation (1) are as follows: pK_B (8.57 at 27°C, 8.55 at 29°C, and salinity of 35) (Dickson, 1990) is the equilibrium constant for boron in seawater; $\alpha_{[B3-B4]}$ is the fractionation factor for isotope exchange between B(OH)$_3$ and B(OH)$_4^-$ in seawater; the δ^{11}B$_{sw}$ (39.61‰) (Foster et al., 2010) and δ^{11}B$_c$ represent the δ^{11}B in seawater and coral, respectively. For this study, we chose the fractionation factor $\alpha_{[B3-B4]}$ of 1.0272 from the empirical study of Klochko et al. (2006), which has been confirmed to be between the coral species-specific values range of 1.026–1.028 (Trotter et al., 2011; McCulloch et al., 2012) and applied in many studies (Allison et al., 2010; Krief et al., 2010; Rollion-Bard et al., 2011; Dissard et al., 2012).

Statistical analyses for this study were completed using the Stats package in R (R Development Core Team, 2013). An assessment of the normality of our data was verified graphically and we used a two-way crossed analysis of variance test (ANOVA) to highlight potential effects of OA, OW, and the interactions between the two factors on coral geochemical composition. When differences were significant, a post-hoc Student's T-test was applied. Mean and standard deviation (or error) are presented.
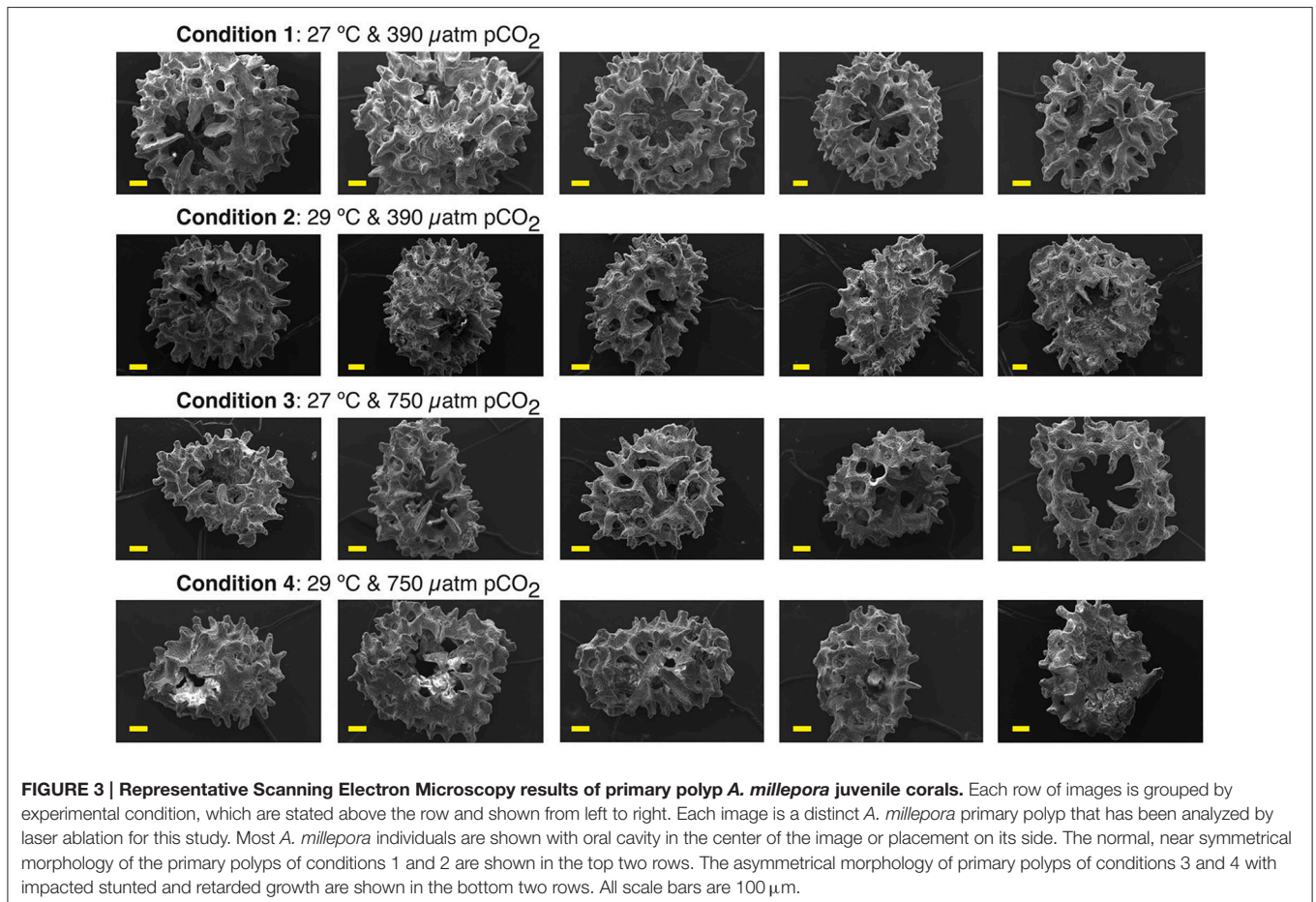
RESULTS AND DISCUSSION

A. millepora Primary Polyp Juvenile Morphology

Visual inspections of our coral juvenile skeletons revealed pronounced morphological differences among the experimental treatments of temperature and pCO_2 (**Figure 2**). As our cultured primary polyp juveniles metamorphosed within the water column, they are different than those found in the field that metamorphosed on settlement substrates. Condition 1 (27°C and 390 μatm pCO_2) and condition 2 (29°C and 390 μatm pCO_2) retained the most symmetrical structure representing normal to near-normal growth (**Figures 2A–D**). Exposure to OW alone (condition 2; **Figures 2C,D**) did not produce skeletal materials that are noticeably different to the control condition (**Figures 2A,B**).

For conditions 3 (27°C and 750 μatm pCO_2) and 4 (29°C and 750 μatm pCO_2), we observed pronounced morphological changes relative to the control. Juveniles of conditions 3 and 4 under OA showed notable stunted asymmetrical growth. The juveniles were notably smaller in overall size with translucent skeletal materials that were brittle and prone to breakage (**Figures 2E–H**). The lack of visual difference between conditions 1 and 2 is likely reflecting the large temperature tolerance range of

this species in nature. In contrast, the asymmetrical growth and microstructure abnormalities of conditions 3 and 4 are common OA stress features in juvenile corals (Cohen et al., 2009; Foster et al., 2015, 2016). With sample picking procedure being equal across all conditions, the brittle and disintegrating nature of the juvenile skeletons under OA and OW is not an artifact of sample handling. Instead, this reflects the inability of the juvenile *A. millepora* coral to build normal skeletons. The findings of the fragile nature of the skeleton and abnormal growth of our coral juveniles are in agreement with previously observed effects on other cultured tropical coral juveniles (Cohen et al., 2009; Foster et al., 2015, 2016).

Scanning Electron Microscopy (SEM) observations confirmed our morphological observations (**Figure 2**) of OA and OW impact on the primary polyps early-life growth stage with more compact or stunted growth leading to smaller overall polyp size (**Figure 3**). *A. millepora* primary polyp calcification at this early-life growth stage in all conditions produced shingle-like aragonite. The proto-aragonite appears prior to the development of the acicular crystals organization, which is interspersed with more developed aragonite crystals. The crystal habit resulted in an aggregate formation resembling fish scale-like morphology, which has been previously described in *Acropora* spp. coral recruits (Gladfelter, 1983, 2007; Van de Locht et al., 2013).

FIGURE 3 | Representative Scanning Electron Microscopy results of primary polyp *A. millepora* juvenile corals. Each row of images is grouped by experimental condition, which are stated above the row and shown from left to right. Each image is a distinct *A. millepora* primary polyp that has been analyzed by laser ablation for this study. Most *A. millepora* individuals are shown with oral cavity in the center of the image or placement on its side. The normal, near symmetrical morphology of the primary polyps of conditions 1 and 2 are shown in the top two rows. The asymmetrical morphology of primary polyps of conditions 3 and 4 with impacted stunted and retarded growth are shown in the bottom two rows. All scale bars are 100 μm.

Centers of calcification (COC or Early Mineralization Zones) and fasciculi (fibrous aragonite) bundles can be observed in all conditions. The COC is the biomineralization structure or setting of coral skeleton that is surrounded by the fibrous aragonite bundles (fasciculi; **Figure 4**). The stunted growth of conditions 3 and 4 resulting from OA impact appears to have reduced or impeded the spread (extension) of the fasciculi between the COCs, creating tighter or more compact assemblages of COC (**Figures 3**, **4**). The abnormal stunted growth at low pH has been shown to be a result of microstructure differences with more COC relative to fasciculi content under high pCO_2 (Hennige et al., 2015). Furthermore, disorganized carbonate precipitation such as disordered aggregate of highly faceted rhombs have been reported (Cohen et al., 2009). Larger spacing between aragonite crystals of the fasciculi can be observed in the primary polyps under OA resulting in more divided aragonite crystals than at ambient pCO_2 (**Figure 4**). Such microstructure changes in the early-life stage of tropical corals have undeniable consequences on the geochemical proxy records as discussed below, in agreement with previous studies (Cohen et al., 2009).

We are aware that since our corals were aposymbiotic or raised without endosymbionts, our morphological observations may have over-simplified the combined effects of elevated CO_2 and temperature change. Various studies with *A. millepora* coral with endosymbionts have shown acclimation possibilities that can range from gene regulation of calcification to metabolism (Strahl et al., 2013; Rocker et al., 2015). Thus, the ability and role of symbiotic zooxanthellae to mitigate *A. millepora* coral stress cannot be discounted. Endo- and ecto-symbionts such as cyanobacteria (Lesser et al., 2004) and microboring algae (Fine and Loya, 2002; Verbruggen and Tribollet, 2011) have also shown notable OA and OW mitigating roles.

δ^{11}B Signature of *A. millepora* Primary Polyp and Reconstructed pH

Mean intra-coral reproducibility for the δ^{11}B ratio ranged between ±0.52 to $\pm0.86‰$ (**Table 3**) and was within the δ^{11}B ratio 2σ SD analytical error. The juvenile *A. millepora* coral δ^{11}B ratio indicates a consistent relationship to the increase in water temperature (**Figure 5A**). Coral juveniles cultured under the same pCO_2 (390 μatm) but different water temperatures had significantly lower mean δ^{11}B ratios at low temperature (27°C, $21.79 \pm 1.61‰$) than high temperature (29°C, $23.41 \pm 0.92‰$; T-test, $p = 1.70 \times 10^{-3}$; **Figure 5A**; **Tables 4, 5**). The same was observed between conditions 3 and 4 cultured under high pCO_2 condition (750 μatm) with significantly lower δ^{11}B ratios at 27°C ($19.18 \pm 2.63‰$) than at 29°C ($22.53 \pm 1.57‰$; T-test, $p = 2.81 \times 10^{-3}$; **Figure 5**; **Tables 4, 5**). The analysis of variance (ANOVA)
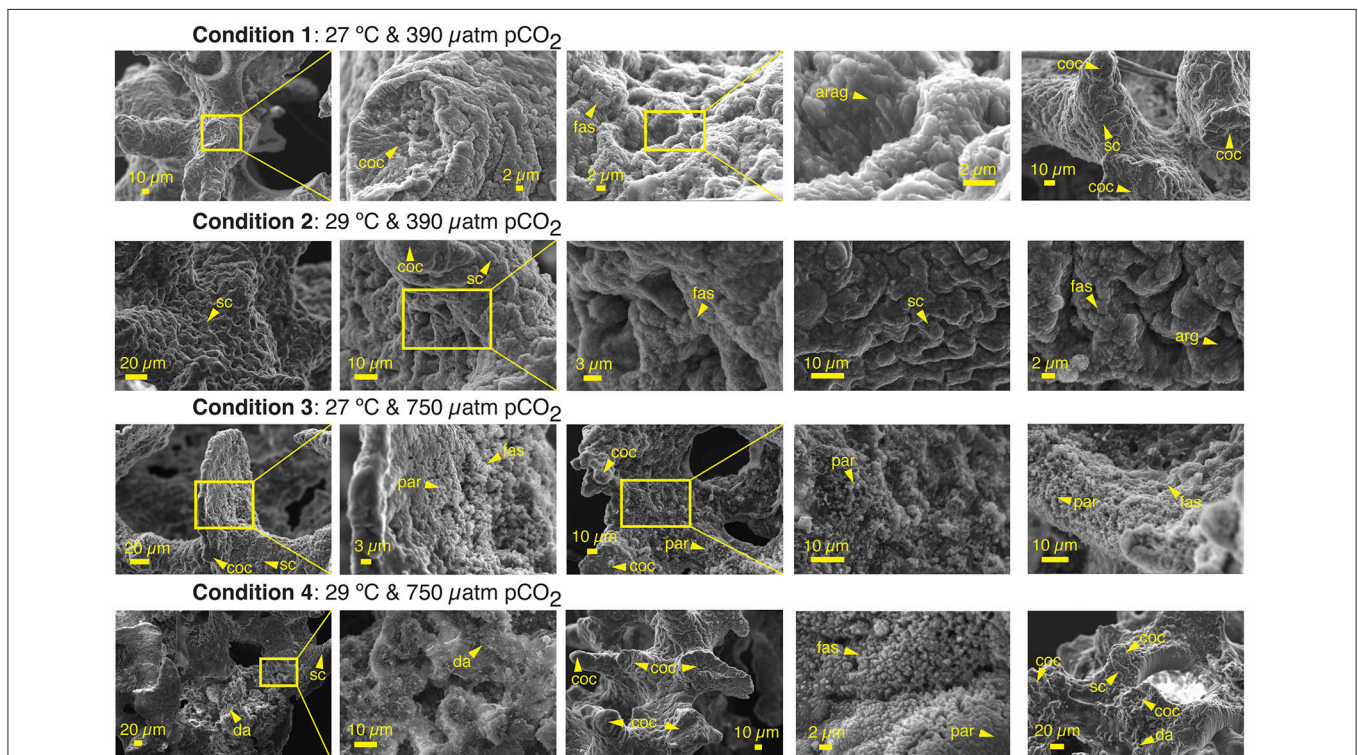

FIGURE 4 | High magnification Scanning Electron Microscopy results of primary polyp *A. millepora* juvenile corals. Each row of images is grouped by experimental condition, which are stated above the row and shown from left to right. Every image is a distinct *A. millepora* primary polyp that has been analyzed by laser ablation for this study. Skeletal microstructure features such as clear centers of calcification (**coc**) and fasciculi bundles (**fas**) composed of primary aragonite crystals (**arag**) can be seen throughout all four experimental conditions. The primary aragonite crystals (**arag**) of the primary polyps are predominantly orientated in a scale-like aragonite formation (**sc**) with newer growth layering on top of older growth. Less developed proto-aragonite (**par**) shingles prior to fine crystals development and presence of disorganized aragonite (**da**) are more prevalent in the OA conditions.

showed that the δ^{11}B ratio was significantly influenced by the expected impact of pCO$_2$ [$F_{(1, 68)}$ = 10.402, p = 2.41 × 10^{-3}] and water temperature [$F_{(1, 68)}$ = 23.895, p = 1.46 × 10^{-5}; **Table 6**].

The estimation of pH (see Section Estimation of Seawater pH and Statistical Analyses; e.g., Zeebe et al., 2001) using the pK_B of 8.57 at 27°C and 8.55 at 29°C (Dickson, 1990), the fractionation factor ($\alpha_{[B3-B4]}$) of 1.0272 (Klochko et al., 2006), and our primary polyp juvenile coral δ^{11}B ratios revealed a pH difference of 0.09

pH units (Total scale) between the control (pH = 8.32) and condition 2 (pH = 8.41). The pH difference is even larger at 0.23 pH units between condition 3 (8.12) and 4 (8.35). The offset between the control condition's reconstructed pH of 8.32 and the measured culture system seawater pH of 7.94 (Total scale converted from the measured pH of 8.08 in NBS scale; **Table 1**) may be due to the choice of boron isotope fractionation factor ($\alpha_{[B3-B4]}$) (Hönisch et al., 2004). But is more likely indicating the difference between seawater and skeletal δ^{11}B and pH variations at the site of calcification or calcification space (Trotter et al., 2011; McCulloch et al., 2012).

TABLE 3 | Primary polyp juvenile *A. millepora* reproducibility in each experimental condition.

Cond.	δ^{11}B (‰)	B/Ca (mmol mol^{-1})	Sr/Ca (mmol mol^{-1})	U/Ca (µmol mol^{-1})
1	±0.86	±0.037	±0.198	±0.083
2	±0.58	±0.037	±0.213	±0.068
3	±0.77	±0.053	±0.162	±0.104
4	±0.52	±0.045	±0.181	±0.085

*Mean intra-coral reproducibility results or test of skeletal homogeneity of each individual primary polyp juvenile coral from three independent laser spot measurements in each experimental condition (Supplementary Figure S1). The experimental conditions can be found in **Table 1**. The number of laser spots per juvenile coral is 3. For δ^{11}B ratios, the total number of juvenile corals analyzed is: Cond. 1 = 10 (n = 30), Condi. 2 = 10 (n = 30), Cond. 3 = 14 (n = 42), and Cond. 4 = 13 (n = 39). For trace elements analyses, the total number of juvenile corals analyzed is: Cond. 1 = 15 (n = 45), Cond. 2 = 22 (n = 66), Cond. 3 = 20 (n = 60), and Cond. 4 = 22 (n = 66).*

TABLE 4 | Summary of mean primary polyp juvenile coral analyses in each experimental condition.

Cond.	δ^{11}B (‰)	B/Ca (mmol mol^{-1})	Sr/Ca (mmol mol^{-1})	U/Ca (µmol mol^{-1})
1	21.79 ± 1.61	0.539 ± 0.052	9.975 ± 0.208	0.954 ± 0.082
2	23.41 ± 0.92	0.531 ± 0.041	9.798 ± 0.162	0.940 ± 0.058
3	19.18 ± 2.63	0.599 ± 0.045	9.674 ± 0.123	1.047 ± 0.068
4	22.53 ± 1.57	0.588 ± 0.039	9.432 ± 0.082	1.008 ± 0.073

*Means of each experimental condition ±1σ standard deviation. The experimental conditions are reported in **Table 1** and the number of primary polyps and laser spots are described in the text and in **Table 3**.*
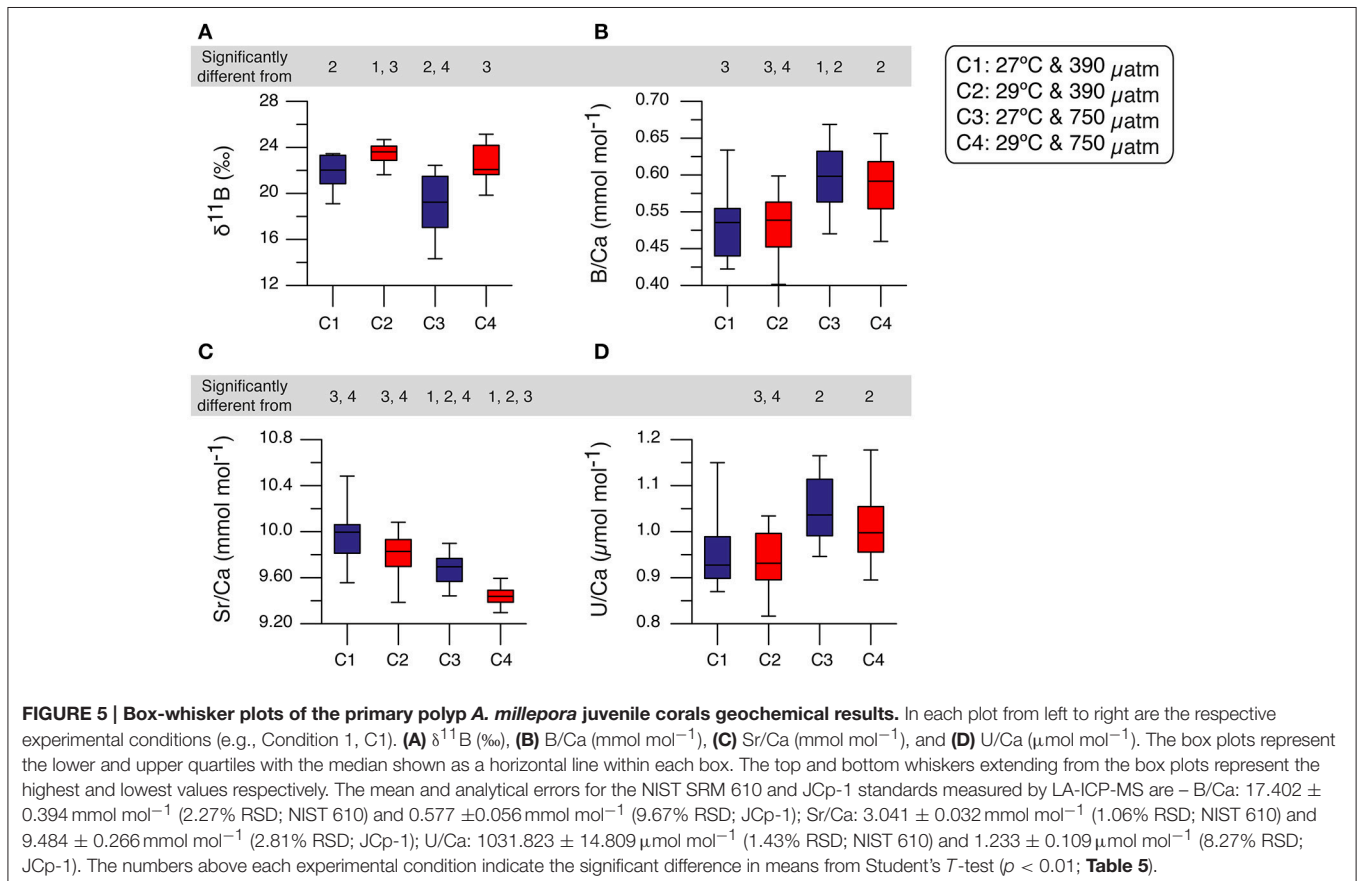

FIGURE 5 | Box-whisker plots of the primary polyp *A. millepora* juvenile corals geochemical results. In each plot from left to right are the respective experimental conditions (e.g., Condition 1, C1). **(A)** δ^{11}B (‰), **(B)** B/Ca (mmol mol^{-1}), **(C)** Sr/Ca (mmol mol^{-1}), and **(D)** U/Ca (µmol mol^{-1}). The box plots represent the lower and upper quartiles with the median shown as a horizontal line within each box. The top and bottom whiskers extending from the box plots represent the highest and lowest values respectively. The mean and analytical errors for the NIST SRM 610 and JCp-1 standards measured by LA-ICP-MS are – B/Ca: 17.402 ± 0.394 mmol mol^{-1} (2.27% RSD; NIST 610) and 0.577 ±0.056 mmol mol^{-1} (9.67% RSD; JCp-1); Sr/Ca: 3.041 ± 0.032 mmol mol^{-1} (1.06% RSD; NIST 610) and 9.484 ± 0.266 mmol mol^{-1} (2.81% RSD; JCp-1); U/Ca: 1031.823 ± 14.809 µmol mol^{-1} (1.43% RSD; NIST 610) and 1.233 ± 0.109 µmol mol^{-1} (8.27% RSD; JCp-1). The numbers above each experimental condition indicate the significant difference in means from Student's *T*-test ($p < 0.01$; **Table 5**).

TABLE 5 | Summary of Student's *T*-test results (*p*-values) between each experimental condition.

Results Cond. 1	Cond. 2	Cond. 3	Cond. 4
$\delta^{11}B$	**1.70e-03**	0.0233	0.1515
B/Ca	0.8407	**9.73e-03**	0.01558
Sr/Ca	0.01373	**1.08e-03**	**3.83e-07**
U/Ca	0.6436	0.01582	0.1494

Results Cond. 2	Cond. 3	Cond. 4	Results Cond. 3	Cond. 4
$\delta^{11}B$	**2.72e-04**	0.04578	$\delta^{11}B$	**2.82e-03**
B/Ca	**1.84e-04**	**1.87e-04**	B/Ca	0.5864
Sr/Ca	**8.93e-03**	**8.98e-08**	Sr/Ca	**5.62e-06**
U/Ca	**5.99e-05**	**1.63e-03**	U/Ca	0.1284

Upper table of the significance of means between condition 1 and experimental conditions 2, 3, and 4. In the bottom left table, the three columns are the significance of means between experimental condition 2 and conditions 3 and 4. The bottom right two columns of the table are the significance of means between conditions 3 and 4. All significant relationships are listed in bold (p < 0.01).

TABLE 6 | Summary of primary polyp juvenile coral two-way (crossed factors) analysis of variance (ANOVA).

	Factor	Sum Sq.	Df	*F*-value	*P*-value
$\delta^{11}B$					
Factor 1	pCO_2	30.553	1	10.4018	**2.41e-03**
Factor 2	Temperature	70.187	1	23.8953	**1.46e-05**
Factors 1 and 2	pCO_2 and Temp.	8.578	1	2.9203	9.47e-02
B/Ca					
Factor 1	pCO_2	0.032684	1	17.8085	**1.24e-04**
Factor 2	Temperature	0.000304	1	0.1658	6.86e-01
Factors 1 and 2	pCO_2 and Temp.	0.000577	1	0.3143	5.78e-01
Sr/Ca					
Factor 1	pCO_2	1.18245	1	43.3953	**5.11e-08**
Factor 2	Temperature	0.54735	1	20.0877	**5.41e-05**
Factors 1 and 2	pCO_2 and Temp.	0.06109	1	2.2419	1.42e-01
U/Ca					
Factor 1	pCO_2	0.043766	1	8.7305	**5.06e-03**
Factor 2	Temperature	0.018059	1	3.6024	6.44e-02
Factors 1 and 2	pCO_2 and Temp.	0.006850	1	1.3663	2.49e-01

Two-way ANOVA of A. millepora juvenile coral geochemical results (n = 47) considered under Factors 1 (pCO$_2$ concentration), 2 (temperature), and the interaction between the two factors (pCO$_2$ and temperature). Sum of Squares (Sum Sq.), Degrees of Freedom (Df), F value, and significance (p-value) are provided. Significant effects (p < 0.01) are shown in bold.

The range of offset, 0.38–0.56 pH units, between skeletal reconstructed pH from our primary polyp juveniles and the surrounding seawater pH is supported by the similarly elevated extracellular pH range (0.2–0.5) measured in coral calcifying space relative to seawater pH in other corals (Venn et al., 2011; McCulloch et al., 2012). Microelectrode pH measurement profiles inside adult polyps of *A. millepora* coral colonies also indicate a 0.5 pH units increase in interior calcification space pH (8.65) relative to seawater pH (8.15) (Cai et al., 2016).

These differences between outside seawater pH and internal calcification space pH are comparable to our reconstructed $\delta^{11}B$-pH and measured seawater pH difference average of 0.43 pH units. Furthermore, high-resolution pH imaging of primary polyp juveniles of aposymbiotic *A. digitifera* indicated active pH up-regulation at the site of calcification (Ohno et al., 2017). Our results confirm these observations in that our coral species also has a well-regulated internal pH at the calcification sites, which is considerably higher than the external seawater pH.

The impact of higher temperature on our *A. millepora* primary polyp resulted in the enrichment of $\delta^{11}B$ causing an increase in reconstructed pH by at least 0.09 pH units (conditions 1 and 2) and 0.23 pH units (conditions 3 and 4). The relationship between temperature and pH at equilibrium is well known, i.e., when the temperature in solution increases, the ability of the water to ionize increases so does the concentration of H^+ ions in solution, leading to a decrease in pH. Without this inherent relationship between temperature and pH, and thus $\delta^{11}B$, the results of conditions 1 and 2 as well as conditions 3 and 4 would have been expected to be more similar with no significant difference between the means. Our observations confirm a previous study with cultured *Acropora* sp. coral nubbins (adult branches) with similar enrichment of skeletal $\delta^{11}B$ ratio due to increasing temperature reflecting behavior changes at the calcification site possibly due to metabolic processes (Dissard et al., 2012). Our microstructure analysis indicates that biomineralization was compromised due to prolonged stress exposure in conditions 3 and 4 (**Figure 4**). The primary polyps of conditions 3 and 4 both contained less bundled (more between crystal spacing) aragonite habits resembling more disorganized orientation of crystals than the conditions at ambient pCO_2. These skeletal features of the primary polyp juveniles may be indicating, in the absence of endosymbionts, the coral only acclimation processes to stress or the attempt to counteract the impact of increased acidification. This response also likely increased the pH up-regulation resulting in a reconstructed pH (8.35, condition 4) that is even more elevated than the control condition (8.32). The enrichment of the $\delta^{11}B$ ratio (conditions 2 and 4), is likely related to metabolic processes of the *A. millepora* juveniles and further support the conclusion that certain coral species have the ability to adapt to increasing OW and OA by up-regulating its internal pH (McCulloch et al., 2012; Ohno et al., 2017). We thus provide additional evidence of pH homeostasis or elevated pH control in scleractinian corals even at the primary polyp juvenile life-stage subjected to OA and OW.

Moreover, a recent study of coral calcifying space pH revealed significant influence and modulation of internal pH due to photosynthesis and respiration (Comeau et al., 2017) that was alluded to by Dissard et al. (2012). The effects of elevated pCO_2 on coral photosynthesis has been reported in previous studies, which have suggested a variety of effects that ranged from inhibitory to stimulatory (Reynaud et al., 2003; Anthony et al., 2008; Kaniewska et al., 2012). Since our primary polyp juveniles were raised without endosymbionts, we are restricted to the discussion of coral animal metabolism or dark respiration. Studies with adult *A. millepora* (Kaniewska et al., 2012) and larvae of *Porites* spp. (Albright and Langdon, 2011; Rivest

and Hofmann, 2014) have all indicated significantly decreased coral respiration due to elevated pCO_2. In adult *A. millepora*, the impact can even be observed prior to biomineralization (Kaniewska et al., 2012). Thus, the metabolic effects of elevated pCO_2 that in turn increased the cost of calcification (McCulloch et al., 2012) cannot be dismissed. This higher cost of calcification is implied from our observations of conditions 3 and 4 that precipitated less fasciculus between the COCs and with more disorganized aragonite aggregation (**Figure 4**). The increase in pCO_2 thus suggests a direct impact of retarded coral calcification related to coral respiration with associated pH up-regulation.

Primary Polyp *A. millepora* Skeletal Sr/Ca as SST proxy

Mean intra-coral reproducibility of the Sr/Ca ratios are within the 1σ SD analytical error of the JCp-1 coral standard (**Table 3**). The difference between Sr/Ca ratio means at low pCO_2 but different temperatures (conditions 1 and 2) was not significant. The large inter-coral Sr/Ca range within these two conditions contributed to this result (**Figure 5**; **Table 4**). Across the high pCO_2 conditions, the mean Sr/Ca ratio of condition 3 (27°C) was significantly higher than condition 4 (29°C; T-test, $p = 5.62 \times 10^{-6}$; **Table 5**). Using published *Acropora* sp. Sr/Ca-SST sensitivity of -0.04 and -0.05 mmol mol^{-1} °C^{-1} (Xiao et al., 2014; Sadler et al., 2016), the 2°C experimental difference between conditions 1 (mean = 9.975 mmol mol^{-1}) and 2 (mean = 9.798 mmol mol^{-1}) would equate to a difference of 3.54 or 4.42°C. Similarly, the difference between conditions 3 (mean = 9.674 mmol mol^{-1}) and 4 (mean = 9.432 mmol mol^{-1}) would equate to a difference of 4.84 or 6.05°C. Our interpretation and discussion are limited by the experimental design consisting of only two temperatures and lacking a full robust temperature calibration range. Nevertheless, the fidelity of the Sr/Ca-SST proxy using *A. millepora* juvenile skeleton at just 2°C warming is uncertain and the results indicate possible bias of reconstructed SST. Even though the Sr/Ca-SST sensitivities used for the *A. millepora* primary polyp juvenile coral may be unsuitable because of the known requirement for species-specific calibrations and possible differences between adults and juveniles. It does however provide a quasi-benchmark on the possibilities for erroneous SST reconstructions using these current Sr/Ca-SST sensitivity calibrations.

Examination of the same temperature (27°C) but different pCO_2 revealed significant difference between the Sr/Ca means of condition 1 and conditions 3 (T-test, $p = 0.0011$; **Figure 5**; **Tables 4, 5**). Likewise, the mean Sr/Ca ratio of condition 2 was significantly different when compared to condition 4 of the same temperature (29°C) but different pCO_2 (T-test, $p = 8.98 \times 10^{-8}$; **Figure 5**; **Tables 4, 5**). These results indicate that the primary polyp juvenile coral Sr/Ca ratio is not only significantly impacted by temperature [ANOVA, $F_{(1, 68)} = 20.088$, $p = 5.41 \times 10^{-5}$; **Table 6**] but also by pCO_2 [ANOVA, $F_{(1, 68)} = 43.395$, $p = 5.11 \times 10^{-8}$; **Table 6**]. The significant impact of OA at 29°C indicates the possibility of inaccurate coral-based SST reconstruction. The difference of 0.37 mmol mol^{-1} between conditions 2 and 4 at 29°C would equate to a difference of $+7.4$ or $+9.2$°C in reconstructed SST due to OA.

Bias of reconstructed SST from coral Sr/Ca under OA has been previously documented (Tanaka et al., 2015; Cole et al., 2016). Our findings of a SST warm bias (low Sr/Ca) between conditions 1 and 3 as well as conditions 2 and 4 are not in agreement with the SST cold bias (high Sr/Ca) results found by Tanaka et al. (2015) and Cole et al. (2016). Studies with cultured Pacific *Porites* spp. and *Acropora digitifera* and Atlantic *Favia fragum* have shown increase in Sr/Ca ratio (colder reconstructed SST) due to increase in pCO_2, declining aragonite saturation, or decrease pH (Cohen et al., 2009; Tanaka et al., 2015; Cole et al., 2016). On the contrary, our results with aposymbiotic *A. millepora* primary polyp revealed a consistent decrease of the Sr/Ca ratio (warming bias) under OA conditions. Biases and inaccuracies in Sr/Ca-SST reconstructions have been attributed to calcification and growth-related factors with suggestions for growth-related rescaling procedures (Gagan et al., 2012). Sr/Ca ratio in corals has also been shown to vary across different skeletal materials and is inherently heterogeneous due to differences in growth (Bagnato et al., 2004; Giry et al., 2010; DeLong et al., 2011).

The microstructure examinations revealing more COC content relative to fasciculi under high pCO_2 cannot explain the decrease in Sr/Ca or reconstructed SST bias because studies have demonstrated that coral COC content results in higher Sr/Ca than fasciculi (Allison et al., 2005; Meibom et al., 2006, 2008). This is in contrast to our geochemical and microstructure findings. Furthermore, we did not observe any secondary aragonite precipitation and dissolution that can alter the Sr/Ca ratio where both of these factors are consistently associated with higher Sr/Ca ratios (cooling bias) (Hendy et al., 2007). Species-specific impact on skeletal Sr incorporation from OA have been observed with no significant impact on *Montipora capitata* Sr/Ca (Kuffner et al., 2012) but significant in other Pacific species (*Porites* spp. and *A. digitifera*) (Tanaka et al., 2015; Cole et al., 2016). Therefore, the bias (lower Sr/Ca) and impact of OA observed in our *A. millepora* primary polyps may be representing hindered early-life stage biomineralization and aragonite precipitation processes.

Relationship of Primary Polyp *A. millepora* Skeletal B/Ca and U/Ca

Mean intra-coral reproducibility of the B/Ca ratio is satisfactory (**Table 3**) and within the 1σ SD analytical error of the JCp-1 coral standard. The primary polyp juveniles cultured at 390 μatm at both temperatures had lower mean B/Ca values than juveniles cultured at 750 μatm at both temperatures (**Figure 5**; **Table 4**). The mean B/Ca of condition 1 (**Figure 5**; **Table 4**) was not significantly different to that in condition 2 (**Table 5**). Mean B/Ca of condition 3 was also not significantly different to that in condition 4 (**Figure 5**; **Tables 4, 5**). The B/Ca ratios did not indicate a temperature effect as observed in the δ^{11}B signature. This is confirmed as our B/Ca ratio was only significantly affected by changes in pCO_2 concentration [ANOVA, $F_{(1, 68)} = 17.808$, $p = 1.24 \times 10^{-4}$; **Table 6**] and not temperature (**Figure 5**; **Table 6**). Our primary polyp juveniles result is in contrast to studies that have found both significant inverse (Fallon et al., 2003) and direct (Dissard et al., 2012) relationships between B/Ca and SST in tropical corals.

Related to the lack of B/Ca correlation to temperature, our primary polyp juvenile corals also do not provide any evidence of a direct relationship between B/Ca and Sr/Ca, contrary to other studies (Sinclair et al., 1998; Fallon et al., 1999; **Figures 6A,B**). Studies using tropical coral species have indeed reported positive correlations between B/Ca and Sr/Ca indicating a coupled relationship to temperature (Fallon et al., 2003; Allison et al., 2010). Comparison to calculated seawater

$[CO_3^{2-}]$ (low $[CO_3^{2-}]$ at high pCO_2 and higher $[CO_3^{2-}]$ at low pCO_2; **Table 1**) support our finding that B/Ca ratios are not significantly different between conditions of the same pCO_2 with different temperatures (**Figure 7A**). It is only significantly impacted by pCO_2 and not water temperature. Instead, our primary polyp juvenile B/Ca results are reflecting the large day-to-day fluctuations of seawater pCO_2 and related $[CO_3^{2-}]$ over the 10-day period (**Table 1**; **Figure 7A**). A recent synthetic
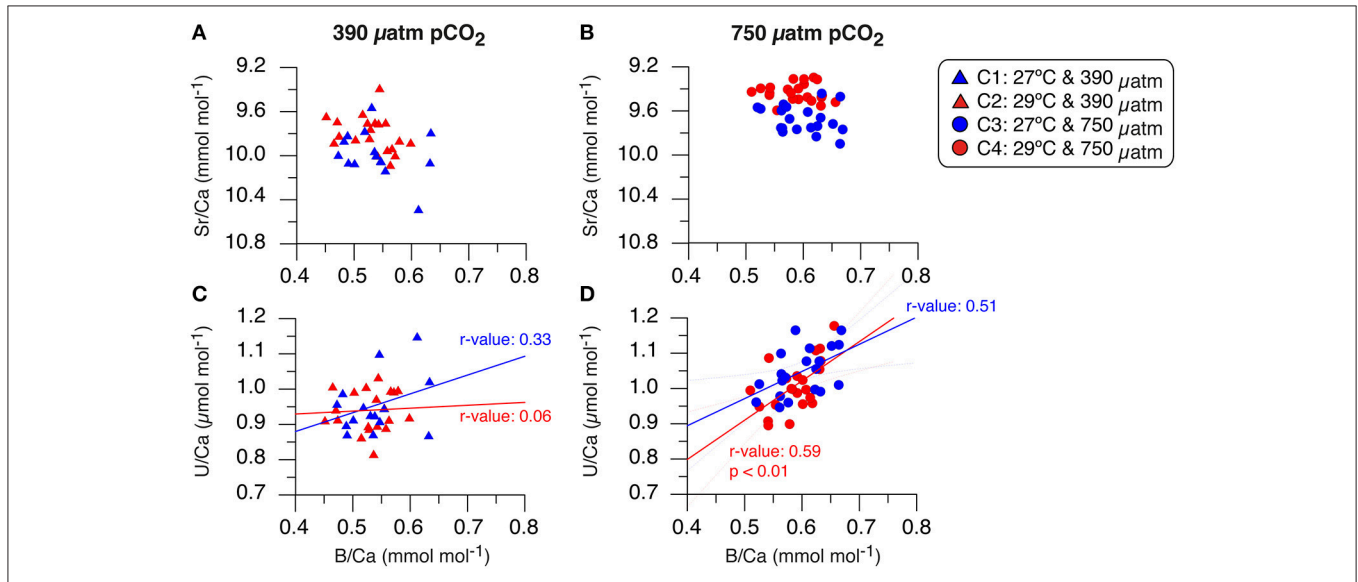
FIGURE 6 | Sr/Ca and U/Ca ratios relationship to B/Ca ratio in primary polyp _A. millepora_ juvenile coral. The Sr/Ca (mmol mol^{-1}) and U/Ca (μmol mol^{-1}) plots are oriented based on pCO_2 concentration with the left column for the experiments at 390 μatm pCO_2 and the right column for the conditions at 750 μatm pCO_2. **(A)** Sr/Ca and B/Ca ratios of condition 1 (blue triangle) and condition 2 (red triangles), **(B)** Sr/Ca and B/Ca ratios of condition 3 (blue circles) and condition 4 (red circles). Note that Sr/Ca ratios are inversely plotted to reflect the temperature relationship of lower (higher) Sr/Ca with higher (lower) temperature. **(C)** U/Ca and B/Ca ratios of condition 1 (blue triangle) and condition 2 (red triangles), **(D)** U/Ca and B/Ca ratios of condition 3 (blue circles) and condition 4 (red circles). Correlation relationships between U/Ca and B/Ca are shown in respective colors with Pearson Product Moment correlation coefficients listed indicating strength of association and significance ($p < 0.01$). The 1σ standard deviation (SD) of the measured NIST SRM 610 and JCp-1 coral standard for trace element/Ca ratios are listed in **Figure 5**.
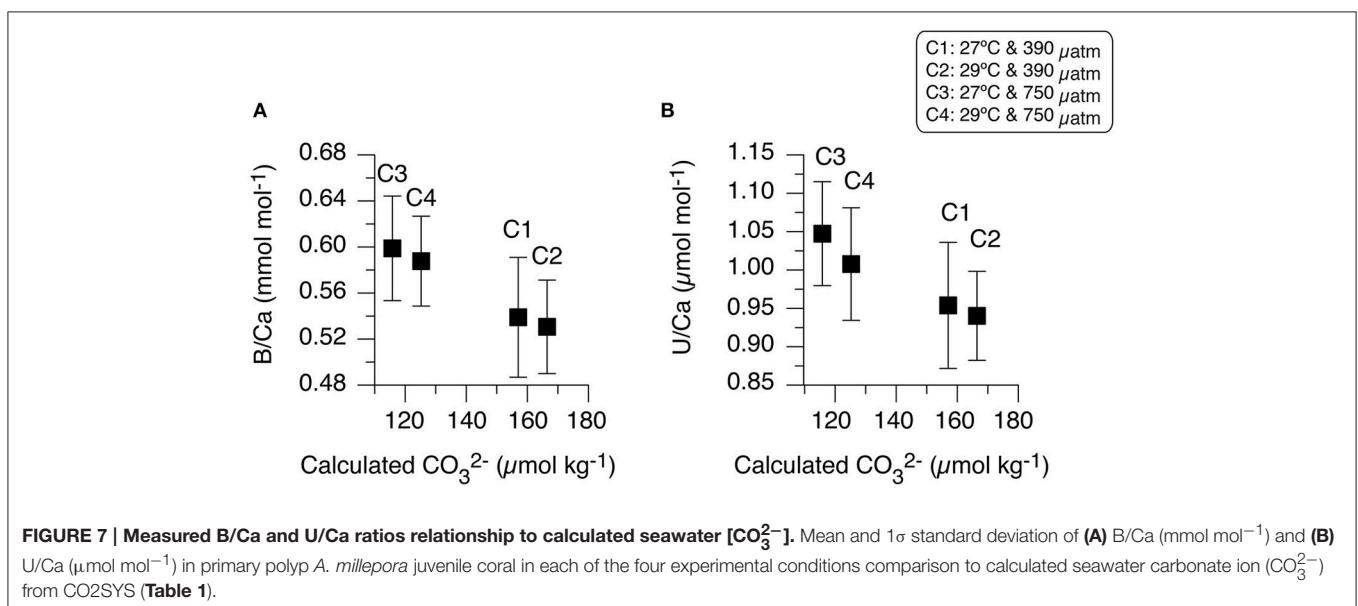
FIGURE 7 | Measured B/Ca and U/Ca ratios relationship to calculated seawater $[CO_3^{2-}]$. Mean and 1σ standard deviation of **(A)** B/Ca (mmol mol^{-1}) and **(B)** U/Ca (μmol mol^{-1}) in primary polyp _A. millepora_ juvenile coral in each of the four experimental conditions comparison to calculated seawater carbonate ion (CO_3^{2-}) from CO2SYS (**Table 1**).

aragonite study corroborates this conclusion since it was demonstrated that aragonite B/Ca ratio can be used to estimate $[CO_3^{2-}]$ as it is principally a function of $[B(OH)_4^-]/[CO_3^{2-}]^{0.5}$ (Holcomb et al., 2016).

Growth and morphological differences may explain the contrast in B/Ca changes related to the variations in microstructure and in proportions of COC and fasciculi. Our B/Ca results (**Figure 5**) are in agreement with morphological observations that under OA conditions, the juvenile coral skeletal materials contain less of the fast growth fasciculi relative to the slower growth COCs and vice versa at ambient pCO_2 (**Figure 4**). Under normal conditions, coral B/Ca ratios are higher in COC than fasciculi in tropical reef corals (Meibom et al., 2006). This is confirmed by our SEM analysis that indicated low pCO_2 conditions produced more visible fasciculi than COCs while OA conditions resulted in more compacted skeletal morphology and decrease in skeletal surface area (less fasciculi and more COC) with disordered aragonite organization. Thus, our result of lower B/Ca ratios is in agreement with skeletal materials containing more fasciculi content relative to COC (Meibom et al., 2006).

Mean intra-coral reproducibility of U/Ca ratios are within the 1σ SD analytical error of the JCp-1 coral standard (**Table 3**). U/Ca ratios in our primary polyp juveniles do not contain a relationship to SST as previous studies have suggested (Min et al., 1995; Cardinal et al., 2001; Armid et al., 2011). In general, the U/Ca ratio was lower (higher) at low (high) pCO_2 (**Figure 5**; **Table 4**). The mean U/Ca of condition 1 was not significantly different than the means of condition 2. It is possible that the 2°C temperature change was within the range of tolerance of *A. millepora*, which did not permit the detection of a temperature effect in U/Ca. Surprisingly, the means of U/Ca in conditions 2 and 3 were not significantly different. In fact, the only mean significance found was between the low means of condition 2 ($0.940 \pm 0.058\,\mu mol\ mol^{-1}$; **Figure 5**) and high means of condition 4 ($1.008 \pm 0.073\,\mu mol\ mol^{-1}$; T-test, $p = 1.63 \times 10^{-3}$; **Table 5**) for cultures at the same elevated temperature (29°C) but different pCO_2.

Of the measured trace elements in the *A. millepora* juvenile coral skeletal material, only U/Ca and B/Ca under high pCO_2 conditions contain occurrence of correlated relationships (**Figures 6C,D**). This is not entirely unexpected as U/Ca in zooxanthellate and azooxanthellate corals have been shown to be influenced by pH (Inoue et al., 2011; Raddatz et al., 2014). Our results partially support this conclusion that the larger change in pCO_2 decrease (increasing OA, decreasing pH) and associated $[CO_3^{2-}]$ induces the only significant impact on U/Ca ratio [ANOVA, $F_{(1,\ 68)} = 8.730$, $p = 0.005$; **Table 6**]. U/Ca in marine biogenic carbonates has been shown to be related to $[CO_3^{2-}]$ of the carbonate system (Russell et al., 2004) and can be explained in terms of uranium speciation in seawater because uranium can easily form complexes with carbonate ions

(Markich, 2002). Thus, the result of increase U/Ca in the primary polyp juvenile skeleton at high pCO_2 conditions comes from a decrease in seawater $[CO_3^{2-}]$ (**Table 1**; **Figure 7B**). Our results suggest the dependence of the two proxies (B/Ca and U/Ca) on seawater $[CO_3^{2-}]$ and therewith calcification rate, which is not merely related to pH or temperature. This may indicate the importance of understanding U/Ca and B/Ca incorporation in coral skeletal materials to deconvolve seawater carbonate chemistry and related equilibrium systems changes.

AUTHOR CONTRIBUTIONS

DD and HW designed the study. HW completed the primary polyps sampling, executed the analytical research and interpretation, and served as primary author. FL, FT, and HW completed the LA-ICP-MS and LA-MC-ICP-MS analyses. DD and AT assisted in data interpretation and writing. AM completed the coral husbandry experimental setup, water measurements, and assisted in writing. ED assisted in the geochemical interpretation and collaborated on the manuscript.

ACKNOWLEDGMENTS

SUPPLEMENTARY MATERIAL

The Supplementary Material for this article can be found online at: http://journal.frontiersin.org/article/10.3389/fmars.2017.00129/full#supplementary-material

REFERENCES

Albright, R., and Langdon, C. (2011). Ocean acidification impacts multiple early life history processes of the Caribbean coral *Porites astreoides*. *Glob. Chang. Biol.* 17, 2478–2487. doi: 10.1111/j.1365-2486.2011.02404.x

Albright, R., Mason, B., Miller, M., and Langdon, C. (2010). Ocean acidification compromises recruitment success of the threatened Caribbean coral *Acropora palmata*. *Proc. Natl. Acad. Sci. U.S.A.* 107, 20400–20404. doi: 10.1073/pnas.1007273107

Allison, N., Finch, A., and EIMF (2010). δ¹¹B, Sr, Mg and B in a modern Porites coral: the relationship between calcification site pH and skeletal chemistry. *Geochim. Cosmochim. Acta* 74, 1790–1800. doi: 10.1016/j.gca.2009.12.030

Allison, N., Finch, A. A., Newville, M., and Sutton, S. R. (2005). Strontium in coral aragonite: 3. Sr coordination and geochemistry in relation to skeletal architecture. *Geochim. Cosmochim. Acta* 69, 3801–3811. doi: 10.1016/j.gca.2005.01.026

Anthony, K. R. N., Kline, D. I., Diaz-Pulido, G., Dove, S., and Hoegh-Guldberg, O. (2008). Ocean acidification causes bleaching and productivity loss in coral reef builders. *Proc. Natl. Acad. Sci. U.S.A.* 105, 17442–17446. doi: 10.1073/pnas.0804478105

Armid, A., Asami, R., Fahmiati, T., Sheikh, M. A., Fujimura, H., Higuchi, T., et al. (2011). Seawater temperature proxies based on DSr, DMg, and DU from culture experiments using the branching coral Porites cylindrica. *Geochim. Cosmochim. Acta* 75, 4273–4285. doi: 10.1016/j.gca.2011.05.010

Bagnato, S., Linsley, B. K., Howe, S. S., Wellington, G. M., and Salinger, J. (2004). Evaluating the use of the massive coral *Diploastrea heliopora* for paleoclimate reconstruction. *Paleoceanography* 19:PA1032. doi: 10.1029/2003PA000935

Baria, M. V. B., Kurihara, H., and Harii, S. (2015). Tolerance to elevated temperature and ocean acidification of the larvae of the solitary corals *Fungia fungites* (Linnaues, 1758). and *Lithophyllon repanda* (Dana, 1846). *Zool. Sci.* 32, 447–454. doi: 10.2108/zs150036

Brand, W. A., Coplen, T. B., Vogl, J., Rosner, M., and Prohaska, T. (2014). Assessment of international reference materials for isotope-ratio analysis (IUPAC technical report). *Pure Appl. Chem.* 86, 425–467. doi: 10.1515/pac-2013-1023

Cai, W., Ma, Y., Hopkinson, B. M., Grottoli, A. G., Warner, M. E., Ding, Q., et al. (2016). Microelectrode characterization of coral daytime interior pH and carbonate chemistry. *Nat. Commun.* 7:11144. doi: 10.1038/ncomms11144

Caldeira, K., and Wickett, M. E. (2003). Anthropogenic carbon and ocean pH. *Nature* 425, 365–365. doi: 10.1038/425365a

Cardinal, D., Hamelin, B., Bard, E., and Pätzold, J. (2001). Sr/Ca, U/Ca and δ¹⁸O records in recent massive corals from Bermuda: relationships with sea surface temperature. *Chem. Geol.* 176, 213–233. doi: 10.1016/S0009-2541(00)00396-X

Chua, C. M., Leggat, W., Moya, A., and Baird, A. H. (2013a). Temperature affects the early life history stages of corals more than near future ocean acidification. *Mar. Ecol. Prog. Ser.* 475, 85–92. doi: 10.3354/meps10077

Chua, C. M., Leggat, W., Moya, A., and Baird, A. H. (2013b). Near-future reductions in pH will have no consistent ecological effects on the early life-history stages of reef corals. *Mar. Ecol. Prog. Ser.* 486, 143–151. doi: 10.3354/meps10318

Cohen, A. L., McCorkle, D. C., De Putron, S., Gaetani, G. A., and Rose, K. A. (2009). Morphological and compositional changes in the skeletons of new coral recruits reared in acidified seawater: insights into the biomineralization response to ocean acidification. *Geochem. Geophys. Geosyst.* 10. doi: 10.1029/2009GC002411

Cole, C., Finch, A., Hintz, C., Hintz, K., and Allison, N. (2016). Understanding cold bias: variable response of skeletal Sr/Ca to seawater pCO₂ in acclimated massive *Porites* corals. *Sci. Rep.* 6:26888. doi: 10.1038/srep26888

Comeau, S., Tambutté, E., Carpenter, R. C., Edmunds, P. J., Evensen, N. R., Allemand, D., et al. (2017). Coral calcifying fluid pH is modulated by seawater carbonate chemistry not solely seawater pH. *Proc. R. Soc. B Biol. Sci.* 284:20161669. doi: 10.1098/rspb.2016.1669

Corrège, T. (2006). Sea surface temperature and salinity reconstruction from coral geochemical tracers. *Palaeogeogr. Palaeoclimatol. Palaeoecol.* 232, 408–428. doi: 10.1016/j.palaeo.2005.10.014

D'Olivo, J. P., McCulloch, M. T., Eggins, S. M., and Trotter, J. (2015). Coral records of reef-water pH across the central Great Barrier Reef, Australia: assessing the influence of river runoff on inshore reefs. *Biogeosciences* 12, 1223–1236. doi: 10.5194/bg-12-1223-2015

De'ath, G., Lough, J. M., and Fabricius, K. E. (2009). Declining coral calcification on the Great Barrier Reef. *Science* 323, 116–119. doi: 10.1126/science.1165283

DeLong, K. L., Flannery, J. A., Maupin, C. R., Poore, R. Z., and Quinn, T. M. (2011). A coral Sr/Ca calibration and replication study of two massive corals from the Gulf of Mexico. *Palaeogeogr. Palaeoclimatol. Palaeoecol.* 307, 117–128. doi: 10.1016/j.palaeo.2011.05.005

Dickson, A. G., and Millero, F. J (1987). A comparison of the equilibrium constants for the dissociation of carbonic acid in seawater media. *Deep Sea Res. A Oceanogr. Res. Pap.* 34, 1733–1743. doi: 10.1016/0198-0149(87)90021-5

Dickson, A. G. (1990). Thermodynamics of the dissociation of boric acid in synthetic seawater from 273.15 to 318.15 K. *Deep Sea Res. A Oceanogr. Res. Pap.* 37, 755–766. doi: 10.1016/0198-0149(90)90004-F

Dissard, D., Douville, E., Reynaud, S., Juillet-Leclerc, A., Montagna, P., Louvat, P., et al. (2012). Light and temperature effects on δ¹¹B and B/Ca ratios of the zooxanthellate coral *Acropora* sp.: results from culturing experiments. *Biogeosciences* 9, 4589–4605. doi: 10.5194/bg-9-4589-2012

Doropoulos, C., Ward, S., Diaz-Pulido, G., Hoegh-Guldberg, O., and Mumby, P. J. (2012). Ocean acidification reduces coral recruitment by disrupting intimate larval-algal settlement interactions. *Ecol. Lett.* 15, 338–346. doi: 10.1111/j.1461-0248.2012.01743.x

Douville, E., Paterne, M., Cabioch, G., Louvat, P., Gaillardet, J., Juillet-Leclerc, A., et al. (2010). Abrupt sea surface pH change at the end of the Younger Dryas in the central sub-equatorial Pacific inferred from boron isotope abundance in corals (*Porites*). *Biogeosciences* 7, 2445–2459. doi: 10.5194/bg-7-2445-2010

Dunbar, R. B., and Wellington, G. M. (1981). Stable isotopes in a branching coral monitor seasonal temperature variation. *Nature* 293, 453–455. doi: 10.1038/293453a0

Eakin, C. M., Lough, J. M., and Heron, S. F. (2009). "Climate variability and change: monitoring data and evidence for increased coral bleaching stress," in Coral *Bleaching: Patterns, Processes, Causes and Consequences*, eds M. J. H. van Oppen and J. M. Lough (Berlin, Heidelberg: Springer), 41–67.

Edmunds, P. J., Brown, D., and Moriarty, V. (2012). Interactive effects of ocean acidification and temperature on two scleractinian corals from Moorea, French Polynesia. *Glob. Chang. Biol.* 18, 2173–2183. doi: 10.1111/j.1365-2486.2012.02695.x

Fabricius, K. E., Langdon, C., Uthicke, S., Humphrey, C., Noonan, S., Okazaki, R., et al. (2011). Losers and winners in coral reefs acclimatized to elevated carbon dioxide concentrations. *Nat. Clim. Chang.* 1, 165–169. doi: 10.1038/nclimate1122

Fallon, S. J., McCulloch, M. T., and Alibert, C. (2003). Examining water temperature proxies in *Porites* corals from the Great Barrier Reef: a cross-shelf comparison. *Coral Reefs* 22, 389–404. doi: 10.1007/s00338-003-0322-5

Fallon, S. J., McCulloch, M. T., van Woesik, R., and Sinclair, D. J. (1999). Corals at their latitudinal limits: laser ablation trace element systematics in *Porites* from Shirigai Bay, Japan. *Earth Planet. Sci. Lett.* 172, 221–238. doi: 10.1016/S0012-821X(99)00200-9

Felis, T., Suzuki, A., Kuhnert, H., Rimbu, N., and Kawahata, H. (2010). Pacific Decadal Oscillation documented in a coral record of North Pacific winter temperature since 1873. *Geophys. Res. Lett.* 37, 2000–2005. doi: 10.1029/2010GL043572

Field, C. B., Barros, V. R., Mach, K. J., Mastrandrea, M. D., van Aalst, M., Adger, W. N., et al. (2014). "Technical summary," in *Climate Change 2014: Impacts, Adaptation, and Vulnerability. Part A: Global and Sectoral Aspects. Contribution of Working Group II to the Fifth Assessment Report of the Intergovernmental Panel on Climate Change*, eds C. B. Field, V. R. Barros, D. J. Dokken, K. J. Mach, M. D. Mastrandrea, T. E. Bilir, M. Chatterjee, K. L. Ebi, Y. O. Estrada, R.C. Genova, B. Girma, E. S. Kissel, A. N. Levy, S. MacCracken, P. R. Mastrandrea, L. L. White (Cambridge; New York, NY: Cambridge University Press), 35–94.

Fine, M., and Loya, Y. (2002). Endolithic algae: an alternative source of photoassimilates during coral bleaching. *Proc. Biol. Sci.* 269, 1205–1210. doi: 10.1098/rspb.2002.1983

Foster, G. L., Hönisch, B., Paris, G., Dwyer, G. S., Rae, J. W. B., Elliott, T., et al. (2013). Interlaboratory comparison of boron isotope analyses of boric acid, seawater and marine CaCO₃ by MC-ICPMS and NTIMS. *Chem. Geol.* 358, 1–14. doi: 10.1016/j.chemgeo.2013.08.027

Foster, G. L., Pogge von Strandmann, P. A. E., and Rae, J. W. B. (2010). Boron and magnesium isotopic composition of seawater. *Geochem. Geophys. Geosyst.* 11. doi: 10.1029/2010GC003201

Foster, T., Falter, J. L., McCulloch, M. T., and Clode, P. L. (2016). Ocean acidification causes structural deformities in juvenile coral skeletons. *Sci. Adv.* 2:e1501130. doi: 10.1126/sciadv.1501130

Foster, T., Gilmour, J. P., Chua, C. M., Falter, J. L., and McCulloch, M. T. (2015). Effect of ocean warming and acidification on the early life stages of subtropical *Acropora spicifera*. *Coral Reefs* 34, 1217–1226. doi: 10.1007/s00338-015-1342-7

Gagan, M. K., Dunbar, G. B., and Suzuki, A. (2012). The effect of skeletal mass accumulation in *Porites* on coral Sr/Ca and δ18O paleothermometry. *Paleoceanography* 27, 1–16. doi: 10.1029/2011PA002215

Gattuso, J., Allemand, D., and Frankignoulle, M. (1999). Photosynthesis and calcification at cellular, organismal and community levels in coral reefs: a review on interactions and control by carbonate chemistry. *Am. Zool.* 39, 160–183. doi: 10.1093/icb/39.1.160

Giry, C., Felis, T., Kölling, M., and Scheffers, S. (2010). Geochemistry and skeletal structure of *Diploria strigosa*, implications for coral-based climate reconstruction. *Palaeogeogr. Palaeoclimatol. Palaeoecol.* 298, 378–387. doi: 10.1016/j.palaeo.2010.10.022

Gladfelter, E. H. (1983). Skeletal development in *Acropora cervicornis* II. Diel patterns of cacium carbonate accretion. *Coral Reefs* 2, 91–100. doi: 10.1007/BF02395279

Gladfelter, E. H. (2007). Skeletal development in Acropora palmata (Lamarck 1816): a scanning electron microscope (SEM). comparison demonstrating similar mechanisms of skeletal extension in axial versus encrusting growth. *Coral Reefs* 26, 883–892. doi: 10.1007/s00338-007-0278-y

Hathorne, E. C., Gagnon, A., Felis, T., Adkins, J., Asami, R., Boer, W., et al. (2013). Interlaboratory study for coral Sr/Ca and other element/Ca ratio measurements. *Geochem. Geophys. Geosyst.* 14, 3730–3750. doi: 10.1002/ggge.20230

Hemming, N. G., and Hanson, G. N. (1992). Boron isotopic composition and concentration in modern marine carbonates. *Geochim. Cosmochim. Acta* 56, 537–543. doi: 10.1016/0016-7037(92)90151-8

Hendy, E. J., Gagan, M. K., Lough, J. M., McCulloch, M., and DeMenocal, P. B. (2007). Impact of skeletal dissolution and secondary aragonite on trace element and isotopic climate proxies in *Porites* corals. *Paleoceanography* 22, 1–10. doi: 10.1029/2007PA001462

Hennige, S. J., Wicks, L. C., Kamenos, N. A., Perna, G., Findlay, H. S., and Roberts, J. M. (2015). Hidden impacts of ocean acidification to live and dead coral framework. *Proc. R. Soc. B Biol. Sci.* 282, 1–10. doi: 10.1098/rspb.2015.0990

Hershey, J. P., Fernandez, M., Milne, P. J., and Millero, F. J. (1986). The ionization of boric acid in NaCl, Na-Ca-Cl and Na-Mg-Cl solutions at 25°C. *Geochim. Cosmochim. Acta* 50, 143–148. doi: 10.1016/0016-7037(86)90059-1

Heyward, A. J., and Negri, A. P. (1999). Natural inducers for coral larval metamorphosis. *Coral Reefs* 18, 273–279. doi: 10.1007/s003380050193

Hoegh-Guldberg, O., Mumby, P. J., Hooten, A. J., Steneck, R. S., Greenfield, P., Gomez, E., et al. (2007). Coral reefs under rapid climate change and ocean acidification. *Science* 318, 1737–1742. doi: 10.1126/science.1152509

Holcomb, M., DeCarlo, T. M., Gaetani, G. A., and McCulloch, M. (2016). Factors affecting B/Ca ratios in synthetic aragonite. *Chem. Geol.* 437, 67–76. doi: 10.1016/j.chemgeo.2016.05.007

Holcomb, M., DeCarlo, T. M., Schoepf, V., Dissard, D., Tanaka, K., and McCulloch, M. (2015). Cleaning and pre-treatment procedures for biogenic and synthetic calcium carbonate powders for determination of elemental and boron isotopic compositions. *Chem. Geol.* 398, 11–21. doi: 10.1016/j.chemgeo.2015.01.019

Hönisch, B., Hemming, N., Grottoli, A., Amat, A., Hanson, G., and Bijma, J. (2004). Assessing scleractinian corals as recorders for paleo-pH: empirical calibration and vital effects. *Geochim. Cosmochim. Acta* 68, 3675–3685. doi: 10.1016/j.gca.2004.03.002

Humphrey, C., Weber, M., Lott, C., Cooper, T., and Fabricius, K. (2008). Effects of suspended sediments, dissolved inorganic nutrients and salinity on fertilisation and embryo development in the coral *Acropora millepora* (Ehrenberg, 1834). *Coral Reefs* 27, 837–850. doi: 10.1007/s00338-008-0408-1

Inoue, M., Suwa, R., Suzuki, A., Sakai, K., and Kawahata, H. (2011). Effects of seawater pH on growth and skeletal U/Ca ratios of *Acropora digitifera* coral polyps. *Geophys. Res. Lett.* 38, 2–5. doi: 10.1029/2011GL047786

Kaniewska, P., Campbell, P. R., Kline, D. I., Rodriguez-Lanetty, M., Miller, D. J., Dove, S., et al. (2012). Major cellular and physiological impacts of ocean acidification on a reef building coral. *PLoS ONE* 7:e34659. doi: 10.1371/journal.pone.0034659

Kleypas, J. A., Buddemeier, R. W., Archer, D., Gattuso, J.-P., Langdon, C., and Opdyke, B. N. (1999). Geochemical consequences of increased atmospheric carbon dioxide on coral reefs. *Science* 284, 118–120. doi: 10.1126/science.284.5411.118

Klochko, K., Kaufman, A. J., Yao, W., Byrne, R. H., and Tossell, J. A. (2006). Experimental measurement of boron isotope fractionation in seawater. *Earth Planet. Sci. Lett.* 248, 276–285. doi: 10.1016/j.epsl.2006.05.034

Krief, S., Hendy, E. J., Fine, M., Yam, R., Meibom, A., Foster, G. L., et al. (2010). Physiological and isotopic responses of scleractinian corals to ocean acidification. *Geochim. Cosmochim. Acta* 74, 4988–5001. doi: 10.1016/j.gca.2010.05.023

Kroeker, K. J., Kordas, R. L., Crim, R. N., and Singh, G. G. (2010). Meta-analysis reveals negative yet variable effects of ocean acidification on marine organisms. *Ecol. Lett.* 13, 1419–1434. doi: 10.1111/j.1461-0248.2010.01518.x

Kuffner, I. B., Andersson, A. J., Jokiel, P. L., Rodgers, K. S., and Mackenzie, F. T. (2008). Decreased abundance of crustose coralline algae due to ocean acidification. *Nat. Geosci.* 1, 114–117. doi: 10.1038/ngeo100

Kuffner, I. B., Jokiel, P. L., Rodgers, K. S., Andersson, A. J., and Mackenzie, F. T. (2012). An apparent "vital effect" of calcification rate on the Sr/Ca temperature proxy in the reef coral *Montipora capitata*. *Geochem. Geophys. Geosyst.* 13, 1–10. doi: 10.1029/2012GC004128

Lazareth, C. E., Guzman, N., Poitrasson, F., Candaudap, F., and Ortlieb, L. (2007). Nyctemeral variations of magnesium intake in the calcitic layer of a Chilean mollusk shell (*Concholepas concholepas*, Gastropoda). *Geochim. Cosmochim. Acta* 71, 5369–5383. doi: 10.1016/j.gca.2007.07.031

Lesser, M. P., Mazel, C. H., Gorbunov, M. Y., and Falkowski, P. G. (2004). Discovery of symbiotic Nitrogen-fixing cyanobacteria in corals. *Science* 305, 997–1000. doi: 10.1126/science.1099128

Lewis, E., and Wallace, D. W. R. (1998). "CO2SYS - Program developed for the CO2 system calculations," in *ORNL/CDIAC-105*, ed Center CDIA (Oak Ridge, TN: Oak Ridge National Laboratory Environmental Sciences Division).

Markich, S. J. (2002). Uranium speciation and bioavailability in aquatic systems: an overview. *Sci. World J.* 2, 707–729. doi: 10.1100/tsw.2002.130

McCulloch, M., Falter, J., Trotter, J., and Montagna, P. (2012). Coral resilience to ocean acidification and global warming through pH up-regulation. *Nat. Clim. Chang.* 2, 623–627. doi: 10.1038/nclimate1473

Mehrbach, C., Culberson, C. H., Hawley, J. E., and Pytkowicx, R. M. (1973). Measurement of the apparent dissociation constant of carbonic acid in seawater at atmospheric pressure. *Limnol. Oceanogr.* 18, 897–907. doi: 10.4319/lo.1973.18.6.0897

Meibom, A., Cuif, J.-P., Houlbreque, F., Mostefaoui, S., Dauphin, Y., Meibom, K. L., et al. (2008). Compositional variations at ultra-structure length scales in coral skeleton. *Geochim. Cosmochim. Acta* 72, 1555–1569. doi: 10.1016/j.gca.2008.01.009

Meibom, A., Yurimoto, H., Cuif, J.-P., Domart-Coulon, I., Houlbreque, F., Constantz, B., et al. (2006). Vital effects in coral skeletal composition display strict three-dimensional control. *Geophys. Res. Lett.* 33, 2–5. doi: 10.1029/2006GL025968

Meyer, E., Aglyamova, G. V., and Matz, M. V. (2011). Profiling gene expression responses of coral larvae (*Acropora millepora*). to elevated temperature and settlement inducers using a novel RNA-Seq procedure. *Mol. Ecol.* 20, 3599–3616. doi: 10.1111/j.1365-294x.2011.05205.x

Min, G. R., Lawrence Edwards, R., Taylor, F. W., Recy, J., Gallup, C. D., and Warren Beck, J. (1995). Annual cycles of U/Ca in coral skeletons and U/Ca thermometry. *Geochim. Cosmochim. Acta* 59, 2025–2042. doi: 10.1016/0016-7037(95)00124-7

Moya, A., Huisman, L., Ball, E. E., Hayward, D. C., Grasso, L. C., Chua, C. M., et al. (2012). Whole transcriptome analysis of the coral *Acropora millepora* reveals complex responses to CO2-driven acidification during the initiation of calcification. *Mol. Ecol.* 21, 2440–2454. doi: 10.1111/j.1365-294X.2012.05554.x

Moya, A., Huisman, L., Forêt, S., Gattuso, J. P., Hayward, D. C., Ball, E. E., et al. (2015). Rapid acclimation of juvenile corals to CO2-mediated acidification by upregulation of heat shock protein and Bcl-2 genes. *Mol. Ecol.* 24, 438–452. doi: 10.1111/mec.13021

Munday, P. L., Dixson, D. L., Donelson, J. M., Jones, G. P., Pratchett, M. S., Devitsina, G. V., et al. (2009). Ocean acidification impairs olfactory discrimination and homing ability of a marine fish. *Proc. Natl. Acad. Sci. U.S.A.* 106, 1848–1852. doi: 10.1073/pnas.0809996106

Nakamura, M., Ohki, S., Suzuki, A., and Sakai, K. (2011). Coral larvae under ocean acidification: survival, metabolism, and metamorphosis. *PLoS ONE* 6:e14521. doi: 10.1371/journal.pone.0014521

Nothdurft, L., and Webb, G. (2007). Microstructure of common reef-building coral genera *Acropora*, *Pocillopora*, *Goniastrea* and *Porites*: constraints on spatial resolution in geochemical sampling. *Facies* 53, 1–26. doi: 10.1007/s10347-006-0090-0

Ohno, Y., Iguchi, A., Shinzato, C., Inoue, M., Suzuki, A., Sakai, K., et al. (2017). An aposymbiotic primary coral polyp counteracts acidification by active pH regulation. *Sci. Rep.* 7:40324. doi: 10.1038/srep40324

Okai, T., Suzuki, A., Kawahata, H., Terashima, S., and Imai, N. (2002). Preparation of a new geological survey of Japan geochemical reference material: coral JCp-1. *Geostand. Newsl.* 26, 95–99. doi: 10.1111/j.1751-908X.2002.tb00627.x

Orr, J. C., Fabry, V. J., Aumont, O., Bopp, L., Doney, S. C., Feely, R. A., et al. (2005). Anthropogenic ocean acidification over the twenty-first century and its impact on calcifying organisms. *Nature* 437, 681–686. doi: 10.1038/nature04095

Palmer, M. R., and Pearson, P. N. (2003). A 23,000-year record of surface water pH and pCO2 in the western equatorial pacific ocean. *Science* 300, 480–482. doi: 10.1126/science.1080796

Pandolfi, J. M., Connolly, S. R., Marshall, D. J., and Cohen, A. L. (2011). Projecting coral reef futures under global warming and ocean acidification. *Science* 333, 418–422. doi: 10.1126/science.1204794

Pearce, N. J. G., Perkins, W. T., Westgate, J. A., Gorton, M. P., Jackson, S. E., Neal, C. R., et al. (1997). A compilation of new and published major and trace element data for NIST SRM 610 and NIST SRM 612 glass reference materials. *Geostand. Newsl.* 21, 115–144. doi: 10.1111/j.1751-908X.1997.tb00538.x

Pelejero, C., Calvo, E., McCulloch, M. T., Marshall, J. F., Gagan, M. K., Lough, J. M., et al. (2005). Preindustrial to modern interdecadal variability in coral reef pH. *Science* 309, 2204–2207. doi: 10.1126/science.1113692

Raddatz, J., Rüggeberg, A., Flögel, S., Hathorne, E. C., Liebetrau, V., Eisenhauer, A., et al. (2014). The influence of seawater pH on U/Ca ratios in the scleractinian cold-water coral *Lophelia pertusa*. *Biogeosciences* 11, 1863–1871. doi: 10.5194/bg-11-1863-2014

R Development Core Team (2013). *R: A Language and Environment for Statistical Computing*. Vienna: R Foundation for Statistical Computing.

Reynaud, S., Leclercq, N., Romaine-Lioud, S., Ferrier-Pagès, C., Jaubert, J., and Gattuso, J.-P. (2003). Interacting effects of CO2 partial pressure and temperature on photosynthesis and calcification in a scleractinian coral. *Glob. Chang. Biol.* 9, 1660–1668. doi: 10.1046/j.1365-2486.2003.00678.x

Ribaud-Laurenti, A., Hamelin, B., Montaggioni, L., and Cardinal, D. (2001). Diagenesis and its impact on Sr/Ca ratio in Holocene *Acropora* corals. *Int. J. Earth Sci.* 90, 438–451. doi: 10.1007/s005310000168

Rivest, E. B., and Hofmann, G. E. (2014). Responses of the metabolism of the larvae of Pocillopora damicornis to ocean acidification and warming. *PLoS ONE* 9:e96172. doi: 10.1371/journal.pone.0096172

Rocker, M. M., Noonan, S., Humphrey, C., Moya, A., Willis, B. L., and Bay, L. K. (2015). Expression of calcification and metabolism-related genes in response to elevated pCO2 and temperature in the reef-building coral *Acropora millepora*. *Mar. Genomics* 24, 313–318. doi: 10.1016/j.margen.2015.08.001

Rodolfo-Metalpa, R., Houlbrèque, F., Tambutté, É., Boisson, F., Baggini, C., Patti, F. P., et al. (2011). Coral and mollusc resistance to ocean acidification adversely affected by warming. *Nat. Clim. Chang.* 1, 308–312. doi: 10.1038/nclimate1200

Rollion-Bard, C., Chaussidon, M., and France-Lanord, C. (2011). Biological control of internal pH in scleractinian corals: implications on paleo-pH and paleo-temperature reconstructions. *Comptes Rendus Geosci* 343, 397–405. doi: 10.1016/j.crte.2011.05.003

Russell, A. D., Hönisch, B., Spero, H. J., and Lea, D. W. (2004). Effects of seawater carbonate ion concentration and temperature on shell, U., Mg, and Sr in cultured planktonic foraminifera. *Geochim. Cosmochim. Acta* 68, 4347–4361. doi: 10.1016/j.gca.2004.03.013

Sadler, J., Nguyen, A. D., Leonard, N. D., Webb, G. E., and Nothdurft, L. D. (2016). *Acropora* interbranch skeleton Sr/Ca ratios: evaluation of a potential new high-resolution paleothermometer. *Paleoceanography* 31, 505–517. doi: 10.1002/2015PA002898

Sadler, J., Webb, G. E., Nothdurft, L. D., and Dechnik, B. (2014). Geochemistry-based coral palaeoclimate studies and the potential of "non-traditional" (non-massive *Porites*). corals: recent developments and future progression. *Earth Sci. Rev.* 139, 291–316. doi: 10.1016/j.earscirev.2014.10.002

Sinclair, D., Kinsley, L., and McCulloch, M. T. (1998). High resolution analysis of trace elements in corals by laser ablation ICP-MS. *Geochim. Cosmochim.* 62, 1889–1901. doi: 10.1016/S0016-7037(98)00112-4

Spivack, A. J., You, C.-F., and Smith, H. J. (1993). Foraminiferal boron isotope ratios as a proxy for surface ocean pH over the past 21 Myr. *Nature* 363, 149–151. doi: 10.1038/363149a0

Strahl, J., Francis, D. S., Doyle, J., Humphrey, C., and Fabricius, K. E. (2013). Biochemical responses to ocean acidification contrast between tropical corals with high and low abundances at volcanic carbon dioxide seeps. *ICES J. Mar. Sci.* 70, 883–891. doi: 10.1093/icesjms/fst034

Tanaka, K., Holcomb, M., Takahashi, A., Kurihara, H., Asami, R., Shinjo, R., et al. (2015). Response of *Acropora digitifera* to ocean acidification: constraints from δ11B, Sr, Mg, and Ba compositions of aragonitic skeletons cultured under variable seawater pH. *Coral Reefs* 34, 1139–1149. doi: 10.1007/s00338-015-1319-6

Thil, F., Blamart, D., Assailly, C., Lazareth, C. E., Leblanc, T., Butsher, J., et al. (2016). Development of laser ablation multi-collector inductively coupled plasma mass spectrometry for boron isotopic measurement in marine biocarbonates: new improvements and application to a modern *Porites* coral. *Rapid Commun. Mass Spectrom.* 30, 359–371. doi: 10.1002/rcm.7448

Tierney, J. E., Abram, N. J., Anchukaitis, K. J., Evans, M. N., Giry, C., Halimeda Kilbourne, K., et al. (2015). Tropical sea-surface temperatures for the past four centuries reconstructed from coral archives. *Paleoceanography* 30, 226–252. doi: 10.1002/2014PA002717

Trotter, J., Montagna, P., McCulloch, M., Silenzi, S., Reynaud, S., Mortimer, G., et al. (2011). Quantifying the pH "vital effect" in the temperate zooxanthellate coral *Cladocora caespitosa*: validation of the boron seawater pH proxy. *Earth Planet. Sci. Lett.* 303, 163–173. doi: 10.1016/j.epsl.2011.01.030

Uppstrom, L. R. (1974). The boron/chlorinity ratio of deep-sea water from the Pacific Ocean. *Deep Sea Res.* 21, 161–162.

Van Achterbergh, E., Ryan, C. G., Jackson, S. E., and Griffin, W. L. (2001). Data reduction software for LA-ICP-MS. Laser-Ablation-ICP-Mass Spectrom. *Earth Sci. Princ. Appl.* 29, 239–243.

Van de Locht, R., Verch, A., Saunders, M., Dissard, D., Rixen, T., Moya, A., et al. (2013). Microstructural evolution and nanoscale crystallography in scleractinian coral spherulites. *J. Struct. Biol.* 183, 57–65. doi: 10.1016/j.jsb.2013.05.005

Venn, A., Tambutté, E., Holcomb, M., Allemand, D., and Tambutté, S. (2011). Live tissue imaging shows reef corals elevate pH under their calcifying tissue relative to seawater. *PLoS ONE* 6:e20013. doi: 10.1371/journal.pone.0020013

Verbruggen, H., and Tribollet, A. (2011). Boring algae. *Curr. Biol.* 21, R876–R877. doi: 10.1016/j.cub.2011.09.014

Watanabe, T., Minagawa, M., Oba, T., and Winter, A. (2001). Pretreatment of coral aragonite for Mg and Sr analysis: implications for coral thermometers. *Geochem. J.* 35, 265–269. doi: 10.2343/geochemj.35.265

Wei, G., McCulloch, M. T., Mortimer, G., Deng, W., and Xie, L. (2009). Evidence for ocean acidification in the Great Barrier Reef of Australia. *Geochim. Cosmochim. Acta* 73, 2332–2346. doi: 10.1016/j.gca.2009.02.009

Xiao, Y., Liu, W., Ma, Y., Zhang, Y., He, M., Luo, C., et al. (2014). Correlation between δ18O, Sr/Ca and Mg/Ca of coral *Acropora* and seawater temperature from coral culture experiments. *Sci. China Earth Sci.* 57, 1048–1060. doi: 10.1007/s11430-013-4710-6

Zeebe, R. E., Sanyal, A., Ortiz, J. D., and Wolf-Gladrow, D. A. (2001). A theoretical study of the kinetics of the boric acid-borate equilibrium in seawater. *Mar. Chem.* 73, 113–124. doi: 10.1016/S0304-4203(00)00100-6